

South Dakota State University

Open PRAIRIE: Open Public Research Access Institutional Repository and Information Exchange

Electronic Theses and Dissertations

2020

Use of Unmanned Aerial System (UAS) for High Throughput Evaluation of Forage Yield in Oat Breeding Nurseries

Prakriti Sharma
South Dakota State University

Follow this and additional works at: <https://openprairie.sdstate.edu/etd>



Part of the [Agronomy and Crop Sciences Commons](#)

Recommended Citation

Sharma, Prakriti, "Use of Unmanned Aerial System (UAS) for High Throughput Evaluation of Forage Yield in Oat Breeding Nurseries" (2020). *Electronic Theses and Dissertations*. 3941.
<https://openprairie.sdstate.edu/etd/3941>

This Thesis - Open Access is brought to you for free and open access by Open PRAIRIE: Open Public Research Access Institutional Repository and Information Exchange. It has been accepted for inclusion in Electronic Theses and Dissertations by an authorized administrator of Open PRAIRIE: Open Public Research Access Institutional Repository and Information Exchange. For more information, please contact michael.biondo@sdstate.edu.

USE OF UNMANNED AERIAL SYSTEM (UAS) FOR HIGH THROUGHPUT
EVALUATION OF FORAGE YIELD IN OAT BREEDING NURSERIES

BY

PRAKRITI SHARMA

A thesis submitted in partial fulfillment of the requirement for the

Master of Science

Major in Plant Science

South Dakota State University

2020

THESIS ACCEPTANCE PAGE

Prakriti Sharma

This thesis is approved as a creditable and independent investigation by a candidate for the master's degree and is acceptable for meeting the thesis requirements for this degree.

Acceptance of this does not imply that the conclusions reached by the candidate are necessarily the conclusions of the major department.

Dr. Melanie Caffè

Advisor

Date

Dr. David Wright

Department Head

Date

Dean, Graduate School

Date

ACKNOWLEDGEMENTS

I would like to thank my academic advisor Dr. Melanie Caffè for this great opportunity to work in interdisciplinary research work. Travelling a long way from home and country for the academic and career opportunity would not been possible without daily guidance, support and encouragement from my advisor. I am blessed for having this life learning experience and opportunity under the direction and mentorship of my advisor.

Special gratitude for South Dakota Crop Improvement Association, South Dakota Agricultural Experiment Station, and the Agronomy, Horticulture, and Plant Science Department for their support.

Also, I am very thankful for Dr. Jiyul Chang, Mr. Larry Leigh for their time, ideas and input over time for this study. Also, my sincere thanks to Jesse Wittnebel and to General Mills for providing me with Unmanned Aerial Systems for this research. I am also thankful for Mr. Mahesh Shrestha (PhD, Image processing), Mr. Basanta Chalise (MS Data Science), Mr. Deepak Raj Joshi (MS, Soil Science) for their continuous guidance and enthusiastic support. I would like to appreciate Nicholas Hall, Koryne Carlson, Krishna Ghimire and Paul Okello for their continuous support for drone flights and field data collection.

Finally, I am highly indebted to my mother (Kamala Sharma), Father (Shreekanta Khatiwada) and brother (Abhikanta Khatiwada) for the love, encouragement and inspiration toward my personal career and academic accomplishment.

TABLE OF CONTENT

ABBREVIATIONS.....	vi
LIST OF FIGURES	vii
LIST OF TABLES	ix
ABSTRACT.....	xii
USE OF UNMANNED AERIAL SYSTEM (UAS) FOR HIGH THROUGHPUT EVALUATION OF FORAGE YIELD IN OAT BREEDING NURSERIES	xii
1. Introduction.....	1
2. Material and Methods	4
2.1. Field experiments.....	4
2.2. Ground data collection.....	5
2.3. Field spectroradiometer measurement	6
2.4. Aerial Platform and Sensors	7
2.5. UAV based data collection	7
2.5.1 Flight dates for year 2018 and 2019	8
2.5.2 Radiometric correction.....	8
2.5.3 Ground Control Points	9
2.6 UAV data processing	9
2.6.1 Image preprocessing	9
2.6.2 Spectral vegetation indices extraction	9
2.7 Statistical analysis.....	11
3. Results and discussions.....	11
3.1 Ground based dry and fresh biomass measurements	11
3.2 Relationships between biomass and other ground-based data.....	13
3.3 Estimation of broad-sense heritability, average and range for the forage and agronomic traits	13
3.4 Relationships between VIs and biomass.....	14
3.4.1 Pearson correlation coefficients between VIs derived from Cropscan and biomass	14
3.4.2 Pearson correlation coefficients between VIs derived from UAV sensors and biomass.....	15
3.5 Relationships between Cropscan and UAV derived vegetation indices	16
3.6 Vegetation index time series for each location.	17
3.6.1 Multispectral VI time series (Micasense)	17
3.6.2 Visual VI time series (RGB sensor).....	18

3.7 Development of models for oat biomass prediction	20
3.7.1 Biomass prediction models using VIs from Slantrange sensor	20
3.7.2 Biomass prediction models using VIs from Micasense sensor.....	21
3.7.3 Biomass prediction models using VIs from RGB sensor	21
3.8 Comparison of VIs extraction methods (average region of interest versus pixel classification)	23
3.8.1 Pearson correlation coefficient between VIs and biomass measure	25
3.8.2 Development of prediction models for oat biomass using VIs derived from the Micasense sensor (Pixel classification method).....	26
4. Conclusion	27
FIGURES	29
TABLES	44
5. References.....	62

ABBREVIATIONS

AOI - Area of Interest

COM - Combination

DN - Digital Number

EXG - Excess Green

EXGR - Excess Green minus Red

GNDVI - Green Normalized Differential Vegetation Index

GPS - Global Positioning System

MLR - Multiple Linear Regression

NDVI - Normalized Differential Vegetation Index

NGRDI - Normalized Green Red Differential Index

RENDVI - Red edge Normalized Differential Vegetation Index

RGB - Red Green Blue

ROI - Region of Interest

RTVI - Red edge Triangular Vegetation Index

SLR - Simple Linear Regression

TVI - Triangular Vegetation Index

UAS - Unmanned Aerial System

UAV - Unmanned Aerial Vehicle

VEG - Vegetation

VI - Vegetative Index

LIST OF FIGURES

Figure 1: Experimental sites in 2019 (South Shore, Volga, Beresford and Pierre) and 2018 (South Shore, Volga, Beresford).....	29
Figure 2: Fresh biomass harvest with forage harvester in Beresford in 2019.	30
Figure 3: Sensors used: Slantrange 2P, Micasense redege and Phantom 4 pro RGB camera (<i>from left to right</i>).	30
Figure 4: Ground control points taken in the field at Beresford.	31
Figure 5: Workflow chart for UAV data processing.	31
Figure 6: Boxplot representing fresh and dry biomass yield (ton per acre) for 35 oat genotypes evaluated at three locations in 2018.....	32
Figure 7: Boxplot representing fresh and dry biomass yield (ton per acre) for 35 oat genotypes evaluated at four locations in 2019.....	33
Figure 8: Boxplot representing the distribution of crown rust severity for 35 oat genotypes evaluated at two locations in 2018.....	33
Figure 9: Boxplot representing the distribution of crown rust severity for 35 oat genotypes evaluated at three locations in 2019.....	33
Figure 10: Bar plot representing the distribution of 14 genotypes selected based on highest crown rust severity rate in 2019.	35
Figure 11: Average NDVI and TVI values derived from imagery collected with a UAV equipped with a Micasense sensor at various dates during the 2019 growing season and coefficient of determination value (R-square) for fresh biomass prediction for 35 oat genotypes grown in Beresford (a), Volga (b) and South Shore (c).	38

Figure 12: Average NGRDI and VEG values derived from imagery collected with a UAV equipped with a RGB sensor at various dates during the 2019 growing season and coefficient of determination value (R-square) for fresh biomass prediction for 35 oat genotypes grown in Beresford (d), Volga (e) and South Shore (f).....	40
Figure 13 a, b, c: Scatterplots of VI (derived from the last flight) by dry and fresh biomass for each sensor types and each location in 2019.....	43
Figure 14: Comparison of pixel under ROI (ROI) and Pixel Classification method (PC) considering correlation coefficient for last flight derived VIs from Micasense with fresh biomass (a) and dry biomass (b).	43

LIST OF TABLES

Table 1: Planting and harvesting dates of the oat forage trials conducted at three locations in 2018 and four locations in 2019.	44
Table 2: Sensors specification.	45
Table 3. Flight dates and sensors used for collecting imagery of the oat forage trials with an unmanned aerial vehicle at each testing site in 2018 and 2019.	46
Table 4. Vegetation indices derived from multispectral sensors	47
Table 5: Vegetation indices derived from visual sensors	48
Table 6: The Pearson correlation coefficient value derived from dry and fresh biomass versus independent variables for 2018.....	49
Table 7: The Pearson correlation coefficient value derived from dry and fresh biomass versus independent variables for 2019.....	49
Table 8: The table representing the range, mean and heritability of forage and agronomic traits in different location for year 2018.	50
Table 9: The table representing the range, mean and heritability of forage and agronomic traits in different location for year 2019.	50
Table 10: Pearson correlation coefficient between VIs from Cropscan sensor and fresh and dry biomass for 35 oat genotypes evaluated at three locations in 2019.....	51
Table 11: Pearson correlation coefficient between VIs derived from the Slantrange sensor and fresh and dry biomass for 35 oat genotypes evaluated at three locations in 2018.	51
Table 12: Pearson correlation coefficient between VIs derived from Micasense and RGB sensor and fresh/dry biomass for 35 different oat genotypes in Volga 2019.....	52

Table 13: Pearson Correlation coefficient VIs derived from Micasense and RGB sensor and fresh/dry biomass for 35 different oat genotypes in Beresford 2019.....	53
Table 14: Pearson correlation coefficient VIs derived from Micasense and RGB sensor and fresh/dry biomass for 35 different oat genotypes in South Shore 2019.....	54
Table 15: Pearson correlation coefficient between VIs from UAV (sensor Mica sense) and VIs from Crop scan in all location for 2019.	55
Table 16: Prediction models for dry biomass harvested from 35 different oat genotypes using VI derived from the Slantrange sensor and agronomic characteristics as predictor variables for 2018. All the model selected on 95% confidence interval and the models not significant are represented as NS	56
Table 17: Prediction models for fresh biomass harvested from 35 different oat genotypes using VI derived from the Slantrange sensor and agronomic characteristics as predictor variables for 2018. All the model selected on 95% confidence interval and the models not significant are represented as NS	57
Table 18: Prediction models for dry biomass harvested from 35 different oat genotypes using VI derived from the Micasense and RGB sensor and agronomic characteristics as predictor variables for 2019. All the model selected on 95% confidence interval and the models not significant are represented as NS	58
Table 19: Prediction models for fresh biomass harvested from 35 different oat genotypes using VI derived from the Micasense and RGB sensor and agronomic characteristics as predictor variables for 2019. All the model selected on 95% confidence interval and the models not significant are represented as NS	58

Table 20: Pearson correlation between VI derived using the pixel classification method from imagery collected with the Micasense sensor and biomass for 35 oat genotypes in 2019.....	60
Table 21: Prediction models for fresh and dry biomass harvested from 35 different oat genotypes using pixel classification method (for Micasense) derived VIs and agronomic characteristics as predictor variables for 2019. All the model selected on 95% confidence interval and the models not significant are represented as NS	61

ABSTRACT

USE OF UNMANNED AERIAL SYSTEM (UAS) FOR HIGH THROUGHPUT
EVALUATION OF FORAGE YIELD IN OAT BREEDING NURSERIES

PRAKRITI SHARMA

2020

Current strategies for phenotyping (for traits like biomass) numerous breeding lines under field conditions demand significant investment in both time and labor. Unmanned aerial systems (UAS) can be used to collect vegetation indexes (VI) with high throughput and could provide an efficient way to predict forage yield in breeding nurseries with accuracy. The main objective of the study was to evaluate the use of VIs derived from UAV collected images for estimating crop biomass. For this study, forage trials consisting of 35 oat genotypes were carried out at three locations in 2018 and four locations in 2019. Unmanned aerial vehicles (UAV) equipped with multispectral and visible sensors were flown over experimental plots in Volga, South Shore, and Beresford, several times throughout the 2018 and 2019 growing seasons. Images were also collected in Pierre in 2019 just prior forage harvest. Fresh and dry biomass were collected on each plot at each location. Several VIs derived from the UAV collected pictures were significantly positively correlated with fresh and dry biomass for the locations Volga and Beresford ($r=0.2-0.65$). However, none of the VIs were significantly correlated with crop biomass in South Shore. Multiple linear regression models (MLR) were developed for each location to predict fresh and dry biomass using VIs, plant height, crown rust severity and chlorophyll content as explanatory variables. The best predictive models for dry

biomass prediction had a R-square value of 0.52 for Volga, 0.67 for Beresford and 0.25 for South Shore. For fresh biomass prediction, selected models had a R-square values of 0.83 for Volga, 0.9 for Beresford, and 0.44 for South Shore. Results from Beresford and Volga suggests that VIs derived from UAV collected could be useful for biomass prediction. Yet, multiple years of trial data would be necessary to further validate the potential use of UAV for estimating oat biomass.

1. Introduction

Oat (*Avena sativa* L.) is a small grain crop, used for direct grazing (Wheeler, 1981), silage, hay and grain production. It is also a beneficial cool season cover crop for biomass production, weed control, erosion control and soil health (Suttie and Reynolds, 2004). In 2018, oats were planted over 290 thousand acres in South Dakota and only 95 thousand acres were harvested for grain (<https://www.nass.usda.gov>). More than 50% of the oats being cultivated in South Dakota are grown for forage.

In comparison to other annual forage crops, oat has a low production and management cost, it performs better in acidic soil conditions, and thrives in variable soil types (<https://plantvillage.psu.edu/topics/oats/infos>). Oat forage is also preferred over other annual forage crops because of its high palatability and dry matter content (Kim, Tinker, & Newell, 2014; McCartney, Fraser, & Ohama, 2008).

Selection for forage yield requires breeding lines to be evaluated in multiple locations for several years. Forage yield is a complex trait controlled by many genes. In recent years, there have been advances in genome sequencing and other molecular technologies (for example; genomic selection, marker assisted selection) that have significantly improved selection procedure and reduced breeding cycle in different types of forage crops (Hayes, 2013). However, for phenotyping forage yield, recent high throughput methodologies still require to be tested and validated for their robustness and cost effectiveness.

Some of the methodologies that are being used for phenotypic assessment of forage yield are visual scoring, sample clipping and mowing of individual breeding plots. The visual scoring method is subjective. The biomass clipping is based on the collection of a small representative sample of the experimental unit which leads to relatively high error on the

estimation of dry matter yield. The mowing procedure for evaluating forage yield consists of harvesting the plots, immediately weighing the biomass and then drying a sub-sample for dry matter yield measurement. These methods are labor intensive and time consuming. Remote sensing platforms like low altitude unmanned aerial systems (UAS) are becoming a common tool to increase the throughput of phenotypic data collection in plant breeding nurseries (Ballesteros et al., 2018; Bendig et al., 2013; Díaz-Varela et al., 2015). UAS are capable of rapid assessment of phenotypes in varietal trials with high spatial and temporal resolution (Shi et al., 2016). UAS platform can be equipped with different types of sensor. Visible and multispectral sensors are commonly used for phenotyping various agronomic traits including yield, disease resistance, ground cover, and biomass.

Above ground biomass can be estimated using VIs. Plant greenness is measured based on reflectance in the near-infrared and visible wavelengths (Gitelson, 2004). The VIs are indicators of actual plant function as leaf or canopy reflectance is dependent on plant status. For example, green vegetation can absorb a large portion of the reflected light spectrum; this is because of the composition of leaf pigments i.e. chlorophyll and xanthophyll. The absorption is directly correlated to the physiological state of plants (Jones and Vaughan, 2010; Marcial-Pablo et al., 2019).

Usually, plant biomass estimation is performed by the calculation of VIs in the near infrared regions (NIR) (Qi et al., 1994; Rouse Jr et al., 1974), which falls under wavelength ranging within 700 and 1300 nm. Spectral indices have been used for biomass prediction in field experiments for various crop species including maize (*Zea mays* L.) (Osborne et al., 2002; Teal et al., 2006) and wheat (*Triticum* spp.) (Babar et al., 2007; Bellairs et al., 1996; Ferrio et al., 2005; Gutierrez et al., 2010; Royo et al., 2003).

One of the most commonly used indices is the normalized difference vegetation index ($NDVI = (NIR-R)/(NIR+R)$) (Calvao and Palmeirim, 2004; Tucker et al., 2001) ; where NIR refers to the reflected value in the near infrared region (800nm) and R refers to the reflected value in the red band region (680nm). NDVI is useful for biomass estimation as it responds to variation in chlorophyll absorption in red spectra and multi scattering in NIR spectra causing high reflectance (Mutanga, 2004). The NDVI has been used for the prediction of biomass and percentage of ground cover in winter forage crops (Prabhakara et al., 2015). However, the use of multiple indices is recommended for biomass prediction as different types of VIs are subject to different sensitivity depending on the amount of biomass and the stage of the crop. The NDVI, GNDVI, SAVI and G-R are more accurate for estimating the biomass at early crop stages (Prabhakara et al., 2015), while they get saturated at later stages (Mutanga and Skidmore, 2004; Thenkabail et al., 2000) and TVI is useful for predicting canopy biomass at later stages (Chen et al., 2009).

Many studies have developed regression models to predict biomass based on spectral reflectance data (Aparicio et al., 2000; Bendig et al., 2014; Brocks and Bareth, 2018). Aparicio et al. (2000) found that NDVI, SR (simple ratio) and PRI (photochemical reflectance index) collected from heading to maturity for durum wheat explained 52, 59 and 39% of the variability in grain yield, respectively. Similarly, Bendig et al. (2014) developed regression models with a R-square value of 0.71 for biomass prediction (using RGB derived VIs and crop surface models) for barley subjected to different nitrogen treatments. Brocks and Bareth (2018) used exponential and simple linear regression models using crop surface models and RGB derived VIs for the prediction of dry biomass in barley (R square value: 0.59,0.77). The use of UAV platforms to estimate biomass in oat breeding

nurseries could be an effective way to address the drawbacks of traditional phenotyping methods for estimating forage yield (Montes et al., 2011). Many breeding lines planted in micro-plots could be quickly evaluated for biomass production at an early stage of line development in a non-destructive manner. While several studies validated the performance of UAS for estimating several important agronomic traits in various crops, the use of UAS for estimating plant biomass in oats hasn't been validated. The main objective of this study is to evaluate the use of VIs derived from UAV collected imagery to predict crop biomass in oat. To achieve these objectives, airborne images (from UAV) and oats dry and fresh biomass was collected from different locations in South Dakota. The predictive performance of various VIs derived from different sensor and with different VI extraction methods were compared in this study.

2. Material and Methods

2.1. Field experiments

For this study, thirty-five oat genotypes, adapted to the Northern Great Plains, were grown at three locations in South Dakota [Volga (44.321994, -96.924565), South Shore (45.105087, -96.927985) and Beresford (43.080859, -96.776148)] in 2018 and 2019. In 2019, an additional site located in central South Dakota was included [Pierre (44.367966, -100.336378)] (Figure1). The experimental design followed a randomized complete block design (RCBD) with three replications. The experimental units were approximately 2.78 m² for Volga, South Shore and Beresford and 6.03 m² for Pierre. Row spacing was 0.19 m. Oats were planted at a density of approximately 300 seeds per square meter and

at a depth of approximately 0.038 m. Homogeneous agronomic management was conducted at each site. The planting and harvesting dates for each location in 2018 and 2019 are provided in Table 1.

2.2. Ground data collection

Several phenotypic traits which could directly or indirectly affect forage yield were collected for this study. During the 2018 growing season, heading date, chlorophyll content, leaf-to-stem ratio, crown rust severity, forage visual rating and plant height were collected. Heading date was recorded for each of individual plot when 50% of the panicles were emerged. Chlorophyll content was measured by using a Chlorophyll meter SPAD-502 Plus (Konica Minolta Sensing Singapore Pte Ltd). The device measures the optical density difference at two wavelengths with an accuracy of +/- 1.0 SPAD units. Measurements were performed on five plants on the first leaf beneath flag leaf. Leaf-to-stem ratio was evaluated on five plants per plot. After removing the roots and panicles, the stem and leaf were separated and placed in an oven set at 70 degree Celsius for one week. The dry weight was then collected, and the leaf-to-stem ratio calculated. Plant height was measured by placing a ruler in the plot and visually estimating the average height (from the ground surface to the tip of the panicles) of all plants in the experimental unit. In 2019, plant height, heading date and crown rust severity were collected. The forage visual rating was given in score of 1-9 depending on the vigor of each plot. When plants were between late milk and early dough, plots were harvested for forage. The plants were cut close to the soil surface with a Jari mower or a forage harvester depending on the location (Figure 2). The fresh weight of each plot was recorded

immediately after harvest. Harvested area was 1.67 square meter at Beresford, Volga, and South Shore in 2018; 2.78 square meter at Beresford, Volga, and South Shore in 2019; and 3.62 square meter in Pierre in 2019. For each plot, a sub-sample was collected and dried in an oven set at 70 degrees Celsius until the weight was stable (approximately a week). Dry matter content was calculated and used to measure dry matter yield for each plot.

$$\text{Dry matter content (\%)}: \frac{\text{Dry sample weight}}{\text{Fresh sample weight}} * 100\%$$

$$\text{Dry biomass: fresh weight} * \text{dry matter content}$$

2.3. Field spectroradiometer measurement

The spectroradiometer measurements were collected for each plot at all locations in 2019 except Pierre. The reflectance spectra were measured using CROPSCAN MSR16R (CROPSCAN Inc, MN 55906 USA) on July 8th in Beresford, July 16th in Volga, and July 18th in South Shore. The CROPSCAN (CROPSCAN Inc., 2013) is a handheld multispectral radiometer which collects spectra between 460 nm and 1640 nm with 16 distinct wave bands. The device consists of two sensors: one for incident light on top of the instrument and one beneath for reflected irradiance from the ground. These two measurements are used to calculate the percent reflectance for each wave band. The CROPSCAN was held approximately 0.5 m above the canopy level. The data was collected only in midday with adequate sun angle and minimum cloud coverage. Irradiance readings below 300 w/m² were deleted to remove inaccuracy caused by cloud cover and insufficient signal-to-noise ratio.

2.4. Aerial Platform and Sensors

The UAVs deployed were a DJI (Dà-Jiāng Innovations) Matrice 600 (SZ DJI Technology Co., Ltd, China) in 2018 and 2019, and a DJI Phantom 4 pro (SZ DJI Technology Co., Ltd, China) in 2019. The DJI Matrice 600 is a six-rotor flying platform, with a maximum takeoff weight of 15.1 kilograms. The DJI Phantom 4 Pro aircraft is a four-rotor flying platform weighing 1.388 kilogram. Both platforms have obstacle sensing technique that helps it to intelligently avoid obstacles during flight. In contrast to the DJI Phantom 4 pro, the DJI Matrice has GPS (Global Positioning System) antenna incorporated in platform itself.

Multispectral images were collected with two different types of sensors. In 2018, the DJI Matrice 600 was equipped with a Sланtrange sensor (Slانtrange, Inc., CA). In 2019, a Micasense sensor (MicaSense, Inc., WA) was used instead on that same platform. The RGB camera which is built-in the DJI Phantom 4 pro was used to collect visual images (Figure 3). The specifications for the three sensors used are provided in Table 2.

2.5. UAV based data collection

For UAV waypoint navigation and flights, autopilot system was applied using Drone Deploy (Drone Deploy, San Francisco, CA) software over AOI (Area of Interest).

Drone deploy software was used for autonomous takeoff, flight and landing purpose, and for capturing consistent data over time. Each of the flight was performed at an altitude of 80 ft and with front and side overlap of 80%. The flight was performed in either full sunny or full cloudy day condition with wind gust less than 12 miles per hour.

2.5.1 Flight dates for year 2018 and 2019

Pictures were collected during multiple flights at each location (Table 3) in June and July (before harvest of biomass at late milk to early dough stage).

2.5.2 Radiometric correction

The Slanrange 2P sensor was equipped with ambient light calibration sensor which was responsible for correcting radiometric error in the raw images. The conversion of digital numbers in raw imageries to reflectance value was performed using Slant View software (see <http://www.slanrange.com/slantview/>). Radiometrically corrected multispectral mosaic images were used to generate various VIs.

In 2019, the radiometric correction was performed using white tarps. Four white tarps were evenly spaced around each corner of each field. The reflectance value of the tarps was determined using the CropScan sensor. The calibration panel was designed following the principles of radiometric calibration i.e. it was spectrally homogeneous, near Lambertian, horizontal, covered a range of reflectance values, and it covered an area many times larger than the pixel size of the sensors used (Smith and Milton, 1999). The four white tarps were used in the development of linear relationship between DN (Digital Number) and surface reflectance. The average DN of white tarps from drone imageries from all the flights were used to develop an equation for each band. The slope and intercept from this linear equation was later used to convert DN values from each band to reflectance. The DN values were converted to reflectance using the following equation:

$$SR_{ij} = \text{Slope} * DN_{ij} \pm \text{Intercept}$$

Where DN_{ij} is the digital number for i^{th} band at j^{th} flight period and SR_{ij} is the surface reflectance for i^{th} band at j^{th} flight period.

2.5.3 Ground Control Points

In order to geo reference the imageries from different flights at the same location, ten ground control points (GCPs) were used across the field area. The GCP coordinates were measured with Magellan GPS device (Magellan Navigation Inc, San Dimas, California). These targets points were considered for all images taken during the growing season to increase accuracy and to overlay measurements taken at the multiple dates for a specific location (Figure 4).

2.6 UAV data processing

2.6.1 Image preprocessing

The processing of raw images captured from UAV was done by using Pix 4D software (Pix4D Inc. San Francisco) to generate orthomosaic images in tiff format. After the initial processing assuring geoinformation, point cloud densification was done for defining the surface of the object and linking related 3D points in images (Figure 5). The orthomosaic images were generated with a spatial resolution of 0.58 cm per pixel for DJI phantom 4, 0.7 cm per pixel in Micasense sensor, and 1.28 cm per pixel for Slantrange sensor.

2.6.2 Spectral vegetation indices extraction

The orthomosaic images were then processed using Arc GIS software (Version 10.7. Redlands, CA) to extract spectral indices. They were first converted to float from raster format. Then, using raster calculator tool in the software, various vegetative indices were created. The shape file was created using the same software and used for the

identification of each breeding plot as an experimental unit. Finally, zonal statistics tools were used to derive vegetation indexes for each experimental unit (Figure 5).

For multispectral images, several VIs were considered including the normalized difference vegetation index (NDVI), green normalized difference vegetation index (GNDVI), and triangular vegetation index (TVI). These VIs are well known for their correlation with biomass. The NDVI is used for prediction of green biomass and changes in vegetation state (Goswami et al., 2015). The GNDVI is sensitive to a wide range of chlorophyll-a concentration ($0.3 - 45 \mu\text{g}/\text{cm}^2$) and could be suitable predictor for biomass at late crop stages (Gitelson et al., 1997). The TVI is known for its reduced effect in asymptotic biomass saturation and was recommended for the estimation of biomass (Prabhakara et al., 2015). The TVI is based on hypothetical triangle in spectral area which links green peak reflectance, maximum chlorophyll absorption and shoulder of NIR band. The red-edge triangulated vegetation index (RTVI) is another index that is used for biomass prediction using reflectance values in NIR, red edge and green spectral bands (Haboudane et al., 2004). The red edge normalized difference vegetation index (RENDVI) is used as a modification of the NDVI for estimating canopy foliage content (Gitelson, 2004) (Table 4).

For RGB images, the indices considered included excess green, excess green minus red, normalized green-red differential index, and vegetiven. These were previously used as predictor variables for the estimation of biomass in barley (Li et al., 2016) and maize (Geipel et al., 2014; Marcial-Pablo et al., 2019) (Table 5).

2.7 Statistical analysis

The relationships between VIs and ground collected data were evaluated using Pearson correlations with “Hmisc” package in R (R core Team 2017). Multiple linear regression models were developed to predict fresh and dry biomass using VIs, plant height, crown rust severity, chlorophyll content, leaf-to-stem ratio and heading date as predictor variables. Two-way ANOVA analysis was performed to see if there is variation in VIs across different genotypes. The regression analyses were performed using SAS studio software. The stepwise selection method was used to select the best predictors. Then, multicollinearity was evaluated by calculating variance inflation factors (VIF) for each selected variable. Variables with a VIF exceeding 10 were excluded to remove collinearity from the model. The models were compared based on their coefficient of determination (R-square) and root mean square error (RMSE).

3. Results and discussions

3.1 Ground based dry and fresh biomass measurements

Thirty-five oat genotypes were evaluated in forage trials at three locations in 2018 and four locations in 2019. The effect of growing environment and genotype on fresh and dry biomass was significant (Table 6 and 7). The highest dry biomass was produced at South Shore with an average of 5.2 and 6.1 tons per acre in 2018 and 2019, respectively (Figure 6 & 7). The lowest dry biomass was produced in Volga with an average of 2.2 and 4.1 tons per acre, in 2018 and 2019, respectively (Figure 6 and 7).

Based on information extracted from the Agacis website, the temperature and precipitation averages at South Shore in 2018 were lower (40.5°F, 21.4 inches) than at Beresford (45.3°F, 36.7 inches) and Volga (42.7°F, 33.9 inches). In 2019, the average temperature during the growing season (May-July) was 61.6°F in South Shore, 66°F in Beresford and 63°F in Volga. In 2019, precipitations during the growing season (May-July) averaged 4.7 inches in South Shore, 3.9 inches in Volga and 4.7 inches in Beresford.

Wet conditions favored the development of crown rust in all three locations.

In 2018, the average crown rust severity was 15.9% in Volga and 44.3% in South Shore (Figure 8). In 2019, crown rust severity was least severe in South Shore. The average crown rust severity was 25 % in South Shore while it was 50% at the other two locations (Figure 9). Not all genotypes had the same level of susceptibility to crown rust. If we observe bar plot in figure 10, the topmost crown rust severity rated genotypes are selected for every location. Hayden and Rockford had highest average severity rate of 85 score in Volga. In Beresford as well, Rockford had the highest average severity rate of 95 score. From the bar plot of South Shore, SD170528 had highest severity rate of 65 score. Since, there was a negative correlation between fresh biomass and crown rust severity at Beresford ($r = -0.59$) and Volga ($r = -0.4$), it suggests that biomass was affected by crown rust at those two locations in 2019. The correlation between biomass and crown rust severity was however not significant in South Shore. (Table 6 and 7).

3.2 Relationships between biomass and other ground-based data

The heading date had significant positive correlation with fresh biomass in Beresford ($r = 0.41$), Volga ($r = 0.47$) and South Shore ($r = 0.33$) in 2018 (Table 6). In 2019, only Pierre had significant positive correlation value of 0.53 between fresh biomass and heading date (Table 7). In 2018, low but significant positive correlations were found between chlorophyll and fresh biomass in Beresford ($r = 0.17$) and Volga ($r = 0.19$) while for South Shore, leaf-to-stem ratio had the moderate positive correlation value of 0.4 with fresh biomass. In 2018, there was no significant correlation between crown rust and biomass at South Shore and Volga (Table 6). In 2019, crown rust severity had significant negative correlation with biomass for Beresford and Volga (Table 7). The plant height was not significantly correlated to fresh or dry biomass in 2018. In 2019, plant height had significant positive correlation with fresh biomass in Beresford ($r = 0.44$), Volga ($r = 0.35$), Pierre ($r = 0.38$) and South Shore ($r = 0.29$). In 2018, the forage visual rating had significant positive correlation with fresh biomass in Beresford (R square = 0.41) and South Shore (R square = 0.27). In 2019, there was no significant correlation between biomass and visual forage rating score with biomass in South Shore.

3.3 Estimation of broad-sense heritability, average and range for the forage and agronomic traits

Broad-sense heritability estimates were calculated for dry and fresh biomass yield and for other agronomic parameters (plant height, heading date, chlorophyll measure, crown rust severity, etc.). For 2018 (Table 8), the broad-sense heritability estimate for fresh biomass

was 0.5 in South Shore, 0.43 in Beresford and 0.35 in Volga. For dry biomass, broad-sense heritability was 0.24 in South Shore, 0.29 in Beresford and 0.03 in Volga. Heading date had the highest broad-sense heritability in Volga ($H^2 = 0.88$) and Beresford ($H^2 = 0.83$). Crown rust severity had heritability estimate of 0.83 in Volga and 0.51 in South Shore. In 2019, broad-sense heritability was relatively higher for fresh and dry biomass in Pierre (fresh: $H^2 = 0.62$ and dry: $H^2 = 0.5$) and in Beresford (fresh: $H^2 = 0.4$ and dry: $H^2 = 0.55$) compared to South Shore (fresh: $H^2 = 0.22$ and dry: $H^2 = 0.35$) and Volga (fresh: $H^2 = -0.03$ and dry: $H^2 = -0.01$). Heading date had the highest broad-sense heritability in Beresford ($H^2 = 0.86$) and in Pierre ($H^2 = 0.89$). In South Shore, broad sense heritability for the crown rust severity was 0.8 which implies that crown rust resistance was mostly influenced by genetic factors (Table 9).

3.4 Relationships between VIs and biomass

Several VIs was derived from multispectral and visual images for each flight in each location (Table 10-14). Pearson correlation coefficients between biomass and the different VIs are shown in Table 10,11,12,13 &14 for Volga, Beresford, and South Shore in 2018 and 2019.

3.4.1 Pearson correlation coefficients between VIs derived from Cropscan and biomass

Multispectral reflectance measurements were collected with a Cropscan on the last flight date at each location (a day before or on the day of forage harvest). Among the VIs collected with the Cropscan, NDVI had the highest correlation with fresh biomass in Volga ($r = 0.65$) and Beresford ($r = 0.75$) (Table 6). NDVI had also the highest

correlation with dry biomass in Volga ($r = 0.48$) and in Beresford ($r=0.63$). None of the VIs derived from the Cropscan were significantly correlated with fresh and dry biomass at South Shore (Table 10).

3.4.2 Pearson correlation coefficients between VIs derived from UAV sensors and biomass

Multispectral reflectance measurements were collected with Slantrange in 2018 and Micasense in 2019 at each location. Among the VIs collected with the Slantrange sensor, GNDVI had the highest correlation with fresh biomass in Volga ($r = 0.5$) and Beresford ($r = 0.49$). However, NDVI had the highest correlation with dry biomass in Volga ($r = 0.48$) and Beresford ($r = 0.43$). There was no significant correlation between VIs and biomass measurements in South Shore (Table 11).

Among the VIs derived from the Micasense sensor (2019), GNDVI had highest correlation with fresh biomass at Volga ($r = 0.49$), Beresford ($r = 0.7$) and South Shore ($r = 0.27$). NDVI was most correlated with dry biomass in Volga ($r = 0.35$), Beresford ($r = 0.55$) and South Shore ($r = 0.2$) (Table 12, 13 and 14).

Among the VIs derived from the RGB sensor (2019), NGRDI had the highest correlation with fresh biomass at Volga ($r = 0.41$), Beresford ($r = 0.61$) and South Shore ($r = 0.21$). NGRDI had the highest correlation with dry biomass in Volga ($r = 0.44$), Beresford ($r = 0.49$) and South Shore ($r = 0.21$) (Table 12, 13 and 14).

In 2018, we had a limited number of flight operations. Consequently, it was difficult to identify the impact of crop development on the accuracy of biomass prediction. In 2019, however, the flights occurred at regular intervals from early vegetative stage till harvest

(June, July). The highest correlation coefficients between crop biomass and VIs occurred at different crop stage for different locations (Table 12, 13 and 14). In Beresford and Volga, the highest Pearson correlation values for multispectral derived VIs and RGB derived VIs were obtained for later flights conducted in July (July, 4th and 11th in Volga, and July 8th and 12th in Beresford) when the majority of the genotypes were at the early dough to dough stage. But in South Shore, a few indices (TVI & RTVI) had significant correlation with biomass for the flight performed on June 25th where many genotypes were at heading stage. However, because the thirty-five genotypes had different maturity, not all plots were at the exact same growth stage when the imagery was collected during each flight.

Overall, among the different types of sensors used in this study (multispectral spectral Cropscan, multispectral Micasense and RGB sensors), the VIs from the Cropscan had the highest correlation coefficients with biomass. Multispectral and RGB sensors had similar performance in term of correlation with biomass for Volga and Beresford. In South Shore, however, irrespective of sensor types, almost none of VIs were significantly correlated to biomass.

3.5 Relationships between Cropscan and UAV derived vegetation indices

The Pearson correlation coefficients were calculated between VIs from Micasense sensor and Cropscan for all locations. The reason behind this comparison was to validate the UAV derived data with broad range multispectral data derived from handheld Cropscan. The VIs extracted from the Micasense multispectral sensor had high correlation value ($r = 0.6-0.78$) with the VIs derived from Cropscan for Beresford. For Volga, the correlation

coefficients ranged from 0.3 to 0.69. For South Shore, RENDVI collected with UAV was most correlated with Cropscan ($r = 0.41$) (Table 15).

3.6 Vegetation index time series for each location

3.6.1 Multispectral VI time series (Micasense)

Change in VIs throughout the growing season were evaluated by plotting average VI by flight date in each environment. This time series analysis was performed for NDVI and TVI index to check for the possibility of saturation of indices (Table 10,11,12) in different environmental conditions.

Changes in average NDVI and TVI (derived from imageries collected with the Micasense sensor) during 2019 growing season are presented for each location in Figure 11 (a, b, and c). For Volga (Figure 11b) and Beresford (Figure 11a), the average NDVI was highest for the last flight date (July 12th in Beresford, July 11th in Volga). For Beresford, the NDVI and TVI collected on the last flight (July 12th) were able to best predict fresh biomass with R-square values of 0.47 and 0.45 respectively. For Volga, the NDVI collected on July 4th were best at predicting fresh biomass with R-square value of 0.26. Whereas, for TVI collected at 25th June flight was best to predict biomass at Volga with R square value of 0.24.

At South Shore (Figure 11c) however, NDVI reached a maximum on June 25th (boot stage). After that, the vegetation index average values decreased with time. A similar trend was observed for coefficient of determination value obtained for NDVI with fresh biomass. For TVI, in other hand, the three flights taken after June 25th had similar average index values.

Also, the average TVI from thirty-five genotypes from imagery collected on June 25th, at boot stage and on July 19th at dough stage were nearly similar. Although, the coefficient of determination for NDVI & TVI with fresh biomass peaked 25th June and was diminishing at later flights.

3.6.2 Visual VI time series (RGB sensor)

Changes in average NGRDI and VEG (derived from imageries collected with the RGB sensor) during the 2019 growing season are presented for each location in Figure 12 (d, e, f). For Volga and Beresford, the average NGRDI was highest at the second to last flight date (July 8th in Beresford, July 11th in Volga). For South Shore, both NGRDI and VEG reached at maximum on July 11th. For Beresford, NGRDI and VEG collected on July 8th were able to best predict fresh biomass with R-square values of 0.5 and 0.34, respectively. However, for South Shore, NGRDI and VEG from flights conducted after June 16th couldn't predict fresh biomass.

One of the possible reasons behind the indices not being able to predict biomass is that they might have been subjected to saturation when the biomass reached a certain threshold value. Index saturation has been reported previously in different studies. (Prabhakara et al., 2015) reported that VIs was not able to detect the amount of biomass when there was a high vegetation for barley and rye. In their study, NDVI, GNDVI, G-R (Green-Red vegetation index) saturated after reaching a value of approximately 0.8 and were only related to biomass under ~1500kg/ha beyond which an increase in biomass did not increase vegetative index value. Index saturation was also reported by Mutanga and Skidmore (2004), where they used narrow band vegetation indices like Modified Normalized Difference Vegetation Index (MNDVI), SR and TVI to estimate biomass of *Cenchrus*

ciliaris. In their study, the standard NDVI showed strong chlorophyll absorption in the red region and near infrared band had lower R square value of 0.26. The SR, MNDVI and TVI were more strongly correlated with biomass (average R-square values of 0.80, 0.77 and 0.77 for SR, MNDVI, and TVI, respectively). Also, in a study done by Hanna et al. (1999), where near-infrared, green and red wavelength bands were used to predict biomass in pasture grasses in the range of 70 to 4000 kg/ha; NDVI was found to be saturated at moderate pasture densities. In our case, average dry biomass was 9,000 kg/ha at the location with the lowest biomass production (Volga) and 13,000 kg/ha at the location with the highest biomass production (South Shore). Therefore, the three sites had biomass higher than the threshold for saturation reported in previous studies.

Another possible cause to explain why VIs were poorly correlated to biomass in South Shore could be nature of the vegetation indices which depend on leaf greenness. The indicator of plant performance in remote sensing is leaf color. This is determined by every genotype with its specific properties like development of chlorophyll, leaf morphological and surface structure etc. These factors are highly affected by environmental stresses and plant nutrition status. In our case, South Shore location having higher moisture and lower temperature might have also affected the biomass production in different genotypes. The presence of dew on the canopies at the time of flight could affect the spectral reflectance measurements and result in inaccurate vegetation indices. Pinter et al. (1986) in their study on the effect of dew on canopy reflectance found that moderate to high dew levels enhanced reflectance in visible wavelengths by 40–60%, and decreased reflectance in wavelengths between 1.15 and 2.35 μm (NIR) by 25–60% in wheat cultivars. Also, for all the locations used in the study were experimentally set up with 35 different genotypes with different

maturity times. The heading stage for all 105 plots in Beresford occurred within 9 days interval, in Volga within 6 days interval and in South Shore within 9 days interval. Therefore, plots had different maturity stage on the day of harvest. There is an evidence that the vegetation indices like NDVI are limited to environmental condition and crop stages (Aparicio et al., 2000). Future studies should include soil moisture status, weather information, crop stage for each genotype and other environmental factors in order to investigate failure of VIs to predict biomass.

3.7 Development of models for oat biomass prediction

The main objective of the study was to estimate fresh and dry biomass using UAV-based VIs. Because chlorophyll content, heading date, plant height, and crown rust severity were sometimes related to oat biomass (Table 6 and 7), those variables were also considered as independent variables to determine if they could improve models for biomass prediction.

3.7.1 Biomass prediction models using VIs from Slantrange sensor

Multiple linear regression models for fresh and dry biomass prediction in 2018 were developed using VIs derived from Slantrange sensor along with several agronomic traits as predictor variables (Table 16 and 17). For dry biomass prediction, models developed with GNDVI and TVI had the best fit for Volga (R-square = 0.35) and Beresford (R-square = 0.3). For South Shore, none of the VIs were able to predict dry biomass.

For estimating fresh biomass, models developed using VIs only had better fit than models developed using agronomic traits only for Volga and Beresford. The models developed

with GNDVI and NDVI had the best fit for Volga (R-square = 0.5) and Beresford (R-square = 0.42). None of the VIs were able to predict fresh biomass for South Shore.

(Table 16 and 17). Models developed using VI derived from imagery collected with the Slantrange sensor had best models with R-square value of 0.35 for dry biomass prediction and 0.5 for fresh biomass prediction. These models have a low predictability for biomass estimation.

3.7.2 Biomass prediction models using VIs from Micasense sensor

Multiple linear regression analysis was done using VIs derived from Micasense sensor as predictor variables for estimating biomass. Prediction models for dry biomass with the best fit had a R-square of 0.58 for Volga, 0.54 for Beresford, 0.22 for South Shore, and 0.17 for Pierre (Table 18).

For fresh biomass (Table 19), the best models had R-square values of 0.6 in Volga, 0.84 in Beresford, 0.2 in South Shore and 0.51 in Pierre.

In all cases, models developed using VIs as predictors variables had higher R-squares and lower RMSE values than models developed using agronomic parameters as predictor variables.

3.7.3 Biomass prediction models using VIs from RGB sensor

Prediction models developed for biomass using VIs derived from the RGB sensor are listed in Table 18 and 19. The best MLR models for dry biomass prediction had R-square values 0.54 for Volga, 0.49 for Beresford and 0.12 for South Shore. (Geipel et al., 2014; Li et al., 2016) reported a stepwise linear regression model for dry biomass prediction with a R-square value of 0.64 when using NGRDI and EXG from RGB sensor and canopy height as

predictor variables. For fresh biomass (Table 19), the best models had R-square values of 0.75 for Volga, 0.73 for Beresford, 0.16 for South Shore. The VIs derived from imagery collected with the RGB sensor were better at predicting biomass than the agronomic data. The advantage of using RGB-based sensor is that imageries have a higher resolution in comparison to those collected with multispectral sensors. The higher resolution helps in visualizing and sorting vegetative and non-vegetative structures (Li et al., 2016). On the other hand, the multispectral sensors have the advantage of having wider wave length enabling to detect NIR spectral information. This has been shown to help in differentiating panicle biomass and green vegetation biomass (Cen et al., 2019).

In this study, both sensor types (Multispectral Micasense and RGB) led to the development of models with similar level of predictability (when comparing R-square and RMSE error). Similar results were found in a study done by Zou et al. (2017), where significant differences between VIs from multispectral (R square = 0.76) and RGB sensor (R-square = 0.73) was not found for estimating yield in rice. Li et al. (2016) used stepwise linear regression with RGB based VIs, mean canopy height, ninety percentile of canopy height, and coefficient of variation of standard and mean canopy height as predictor variables for estimating aboveground biomass of maize. Their best model was able to predict above ground biomass with a R-square of 0.64. Their result is like our regression models using RGB based VIs and other variables; the best models for fresh biomass prediction had a R-square of 0.73 for Beresford and 0.75 for Volga. One of the studies developed regression models for above ground biomass in wheat using RNDVI, GNDVI, SR and WI (Water Index) as predictor variables. Their models accounted for 79, 85, 93 and 87 % of the variation in the aboveground biomass yield of wheat (Grain, 2014). In our case, prediction

models based on VIs from multispectral sensors explained 60% and 84% of the total variation in fresh biomass in Volga and Beresford. However, neither the VIs from multispectral sensor nor the VIs from the RGB sensors were not able to give accurate biomass estimation for South Shore (only 20% of variation in fresh biomass was explained).

The performance of VIs from RGB and multispectral sensors in predicting biomass varied with the location and the type of biomass (fresh or dry). In Beresford, NDVI from the multispectral sensor resulted in higher coefficient of determination values for biomass prediction compared to NGRDI from RGB sensor (Figure 13 a). For Volga, NGRDI derived from the RGB sensor had higher coefficient of determination values for biomass prediction than NDVI derived from the multispectral sensor (Figure 13 b). Whereas for South Shore, VIs from either sensor resulted in non-significant coefficient of determination value ($R\text{-square} < 0.1$).

3.8 Comparison of VIs extraction methods (average region of interest versus pixel classification)

For the analyses reported in previous sections, VIs extraction through Arc GIS was done by selecting the region of interest (ROI) for each experimental plot. Average spectral reflectance of each band was calculated using all the pixels that fell within the ROI. However, pixels in the ROI included shadows, background soil, and panicles (after heading), which could affect the overall VIs values. Since, spectral indices are very

sensitive to green living vegetation, it is essential to select pixels with high NIR reflectance as a representative of green pixels from ROI.

Several studies (Booth et. al 2006, Patrignani et. al 2015) used pixel classification to enhance the accuracy of UAV based data to differentiate canopy and non-canopy area. Booth et.al (2006) used single pixel sample point method to differentiate shrub and grass species from other background pixels. Patrignani et. al (2015), used Canopeo (automatic color threshold classification in MATLAB (The Mathworks, Inc., Natick, MA, USA) which classified pixels to canopy and non-canopy categories in various crops (turf, corn, sorghum, etc.). Schirrmann et.al (2016), in his research to estimate biomass in wheat, found that K-mean clustering algorithm is a faster method for pixel classification and more accurate when applied to clustering based on spectral reflectance of NIR rather than VIs like NDVI.

For our study, MATLAB was used for K-mean clustering procedure using stacked mosaic images to create 6 cluster classes. This differentiation of cluster is based on the color feature of the image. Based on higher NIR reflectance, cluster types with green pixels were identified. A binary vegetation image was created after masking non canopy type cluster class. Then DN values for that cluster was extracted for all bands (NIR, red edge, red, green and blue) and converted to surface reflectance using calibration method. This was done for 2019 imageries collected with the Micasense sensor and the same vegetation indices (NDVI, GNDVI, RENDVI, TVI & RTVI) were re-extracted.

3.8.1 Pearson correlation coefficient between VIs and biomass measure

In comparison with the standard method of deriving VIs using all pixels in the ROI, pixel classification resulted in VIs more highly correlated with biomass in certain cases. For the last flight in Beresford, the correlation between fresh biomass and NDVI was $r = 0.69$ for the average pixel method and $r = 0.71$ after pixel classification. For the last flight in Volga, the correlation between fresh biomass and NDVI was $r = 0.47$ for the average pixel method and $r = 0.74$ after pixel classification.

Similarly, for the last flight in Beresford, the correlation between dry biomass and NDVI was $r = 0.55$ for the average pixel method and $r = 0.56$ after pixel classification. For the last flight in Volga, the correlation between dry biomass and NDVI was $r = 0.35$ for the average pixel method and $r = 0.55$ after pixel classification.

The two methodologies gave similar results for Beresford. For Volga, however, the pixel classification method resulted in higher correlation between biomass and certain VIs. Also, it is important to note that the changes in correlation coefficient values are inconsistent depending on the vegetation index (Figure 14a). GNDVI was the most correlated to fresh biomass prediction in Volga with the average pixel under ROI method, whereas NDVI was the most highly correlated with fresh biomass at that location with the pixel classification method. For that same location, the correlation between dry biomass and RENDVI was drastically increased when the pixel classification method was used in comparison to the average pixel method.

No differences were observed between the two methods for South Shore. In both cases hardly any vegetation index appeared to have significant correlation to biomass. The RENDVI vegetation index had correlation of 0.31 with fresh biomass and GNDVI had correlation of 0.27 with dry biomass for pixel classification method. (Figure 14 a & b).

3.8.2 Development of prediction models for oat biomass using VIs derived from the Micasense sensor (Pixel classification method)

Table 20 lists the MLR models developed with VIs extracted using the pixel classification method (Micasense sensor). The best models for dry biomass prediction had a R-square value of 0.52 in Volga, 0.67 in Beresford and 0.25 in South Shore. For fresh biomass prediction, selected models had a R-square values of 0.83 in Volga, 0.9 in Beresford, and 0.44 in South Shore.

Overall models developed using VIs derived through pixel classification had a better fit for predicting fresh biomass than models developed using VIs derived through the average pixel under ROI method .For all locations, predictive models for fresh biomass derived using only VIs derived using the pixel classification method had R-square values higher than models based on VIs derived using the average pixel under ROI method (Table 21).

Nevertheless, the results were different for dry biomass. For dry biomass prediction in Volga, using the pixel classification method resulted in a model with a R-square value of 0.48 while the average pixel under ROI method resulted in a model with a R-square value

of 0.56. The relative performance of these methods for VI extraction depended on the location.

Myneni and Williams (1994), when considering different planophile and erectophile species, reported that NDVI was unaffected by pixel heterogeneity for estimating canopy vigor based on biomass and color. Similarly, to our study, Tremblay et al. 2014 reported that the use of the pixel classification method barely increased the correlation between fresh biomass and leaf area index in corn as well as between fresh biomass and soil adjusted vegetation index (SAVI) using multispectral imagery derived from UAV.

4. Conclusion

The purpose of the study was to estimate oat biomass using VIs derived from high resolution imageries. Differences in growing conditions between the three locations resulted in significant variation in oat biomass production. In Beresford, where susceptible cultivars were affected by severe crown rust infections, a significant negative correlation between crown rust severity and biomass was observed.

The VIs derived from multispectral and RGB sensors were found to be positively correlated to fresh and dry biomass in Volga and Beresford. However, the strength of the correlation between vegetation indices and oat biomass were dependent on the environmental conditions. The VIs was more highly correlated with fresh biomass than with dry biomass. In South Shore, very few UAV derived VIs was significantly correlated with biomass. The different sensors types (Micasense, RGB, Cropscan) gave similar results for South Shore. There could be several reasons behind the failure of VIs

to predict oat biomass at this location which needs to be further investigated in future studies.

Several predictive models for estimating biomass were developed using VIs from UAV imagery. Including agronomic parameters (such as crown rust severity rating, plant height, etc.) in the predictive models didn't improve model fit as compared to models developed using VIs only. This suggests that UAV imagery derived data could be used as a potential measure to estimate oat biomass in oat forage breeding program.

Two different methodologies for VI extraction were compared i.e. pixel classification method and average pixel value under ROI method. The pixel classification method was applied using K-mean cluster algorithm. The differences between correlation coefficient value derived from VIs and biomass from pixel classification method and pixel under ROI method was inconsistent comparing to locations. For Volga, VIs derived using the pixel classification method had much higher correlation coefficient value with biomass compared to average pixel under the ROI method. However, in South Shore and Beresford, the results were similar for both methods. The inconsistent results observed depending on the location suggests that additional years of data would be necessary to further evaluate the potential use of UAV for estimating oat biomass.

FIGURES

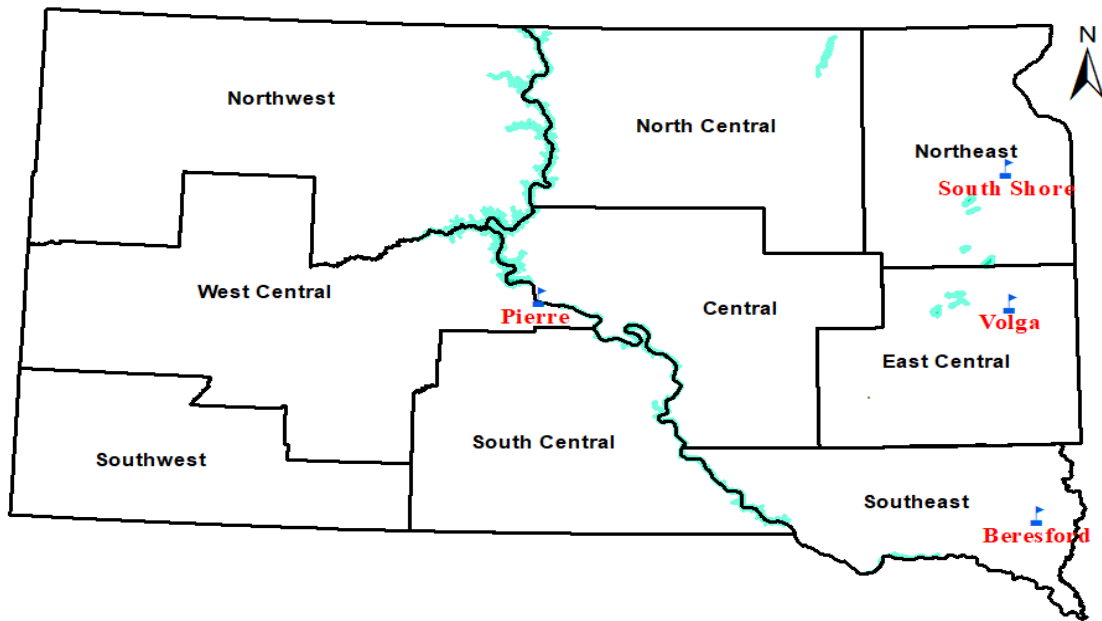


Figure 1: Experimental sites in 2019 (South Shore, Volga, Beresford and Pierre) and 2018 (South Shore, Volga, Beresford).



Figure 2: Fresh biomass harvest with forage harvester in Beresford in 2019.



Figure 3: Sensors used: Slanrange 2P, Micasense rededge and Phantom 4 pro RGB camera (*from left to right*).



Figure 4: Ground control points taken in the field at Beresford.

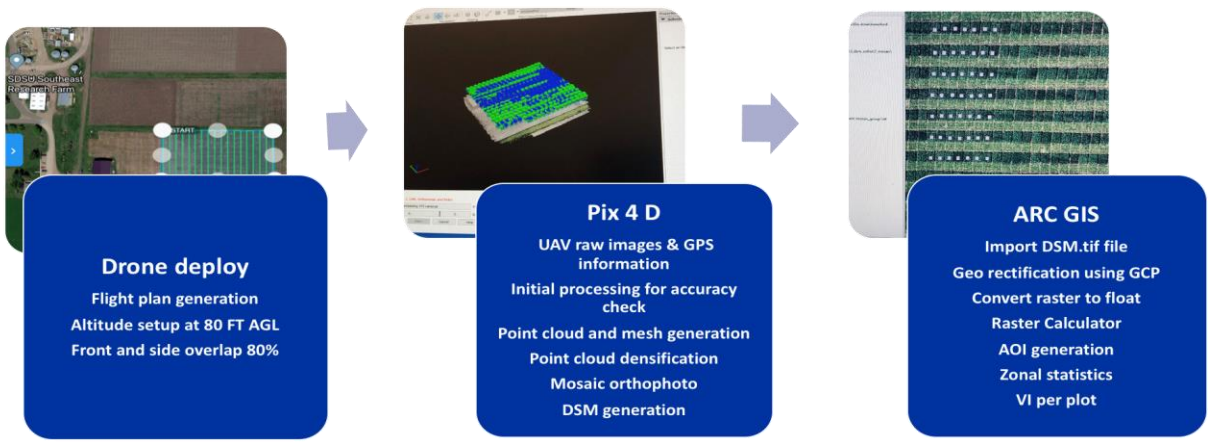


Figure 5: Workflow chart for UAV data processing.

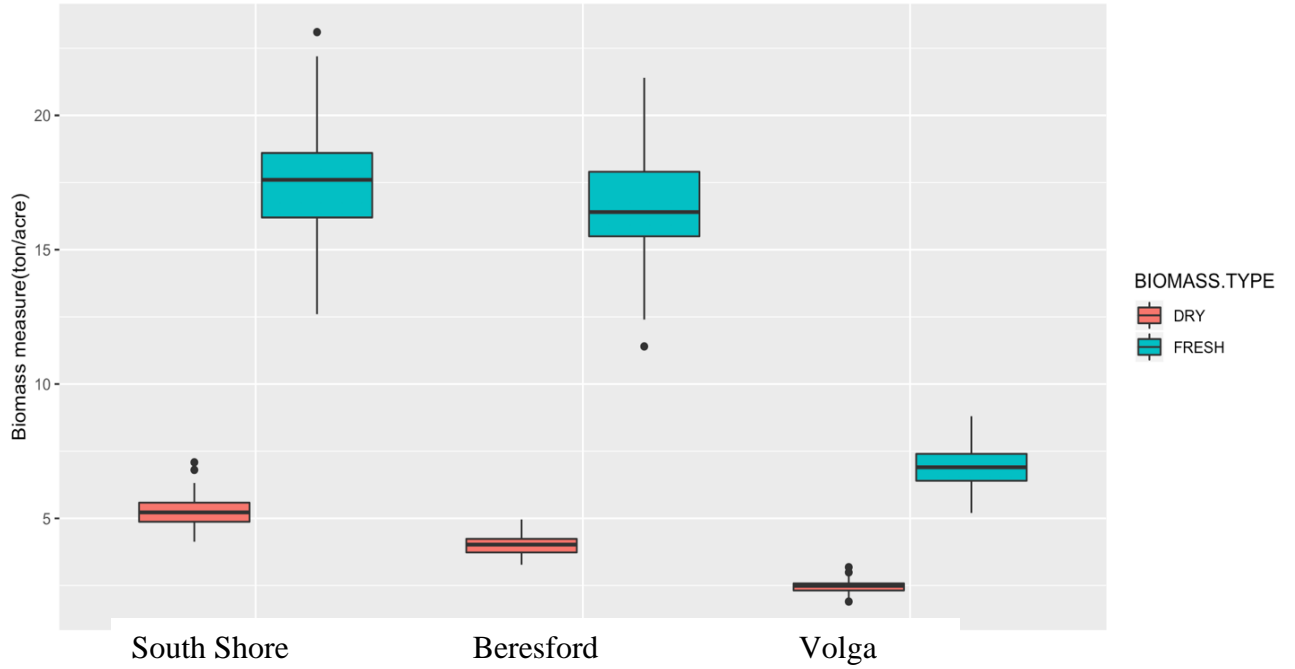


Figure 6: Boxplot representing fresh and dry biomass yield (ton per acre) for 35 oat genotypes evaluated at three locations in 2018.

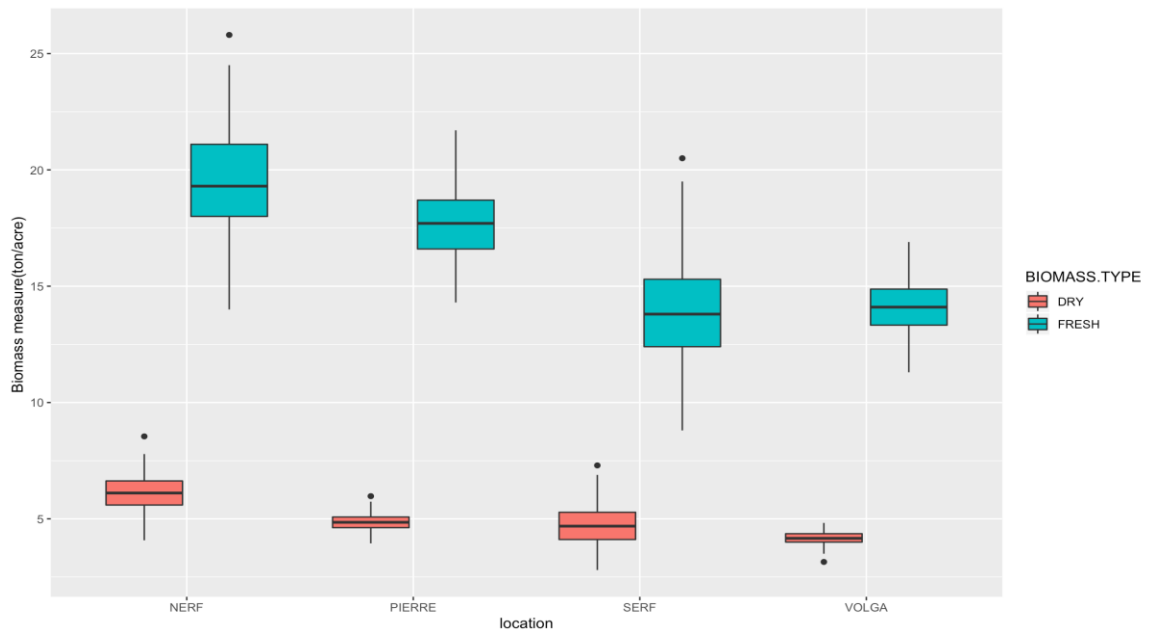


Figure 7: Boxplot representing fresh and dry biomass yield (ton per acre) for 35 oat genotypes evaluated at four locations in 2019.

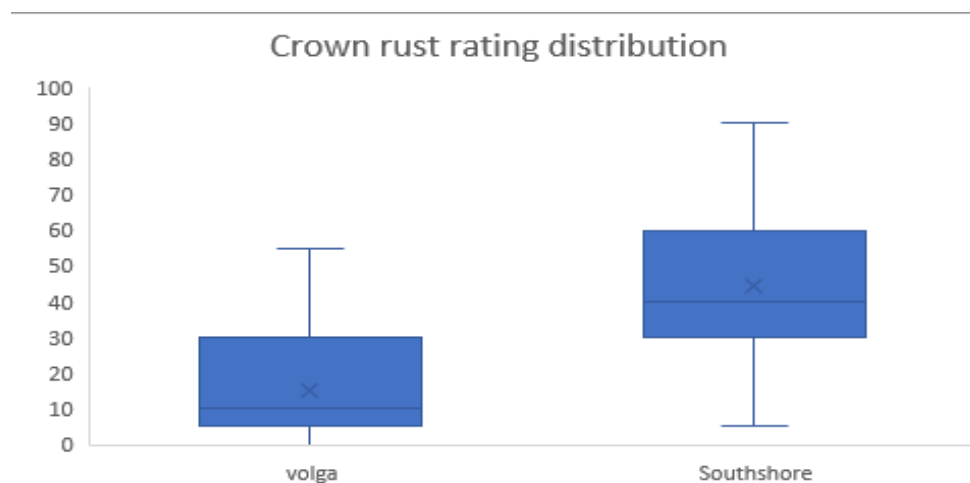


Figure 8: Boxplot representing the distribution of crown rust severity for 35 oat genotypes evaluated at two locations in 2018.

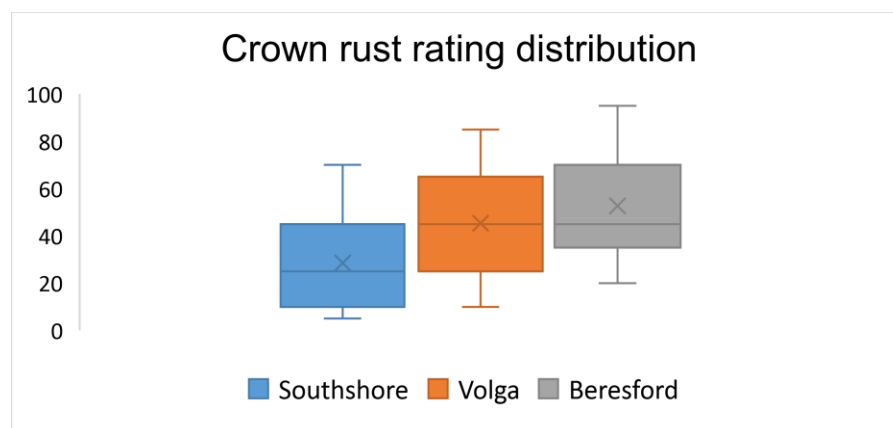
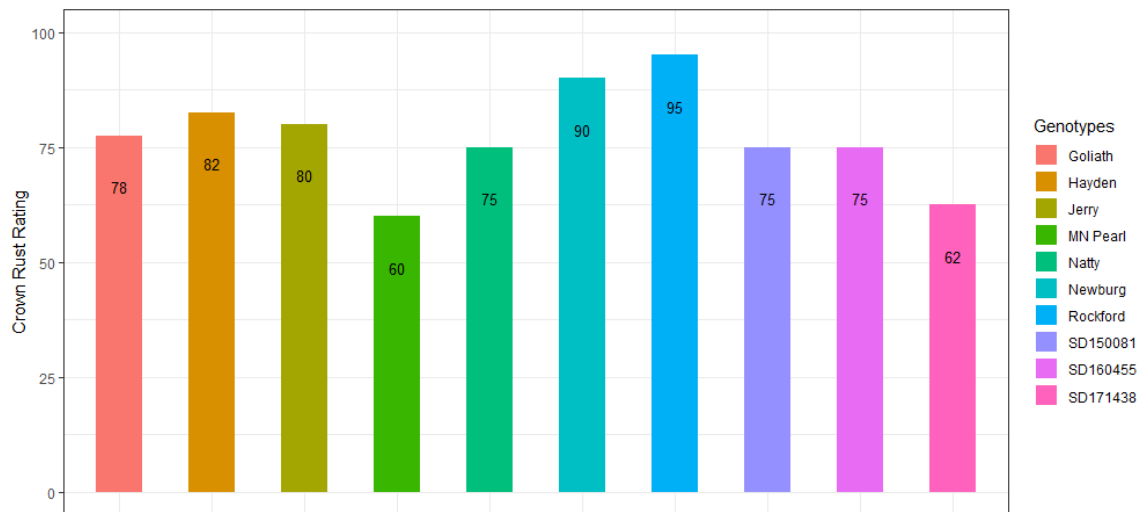
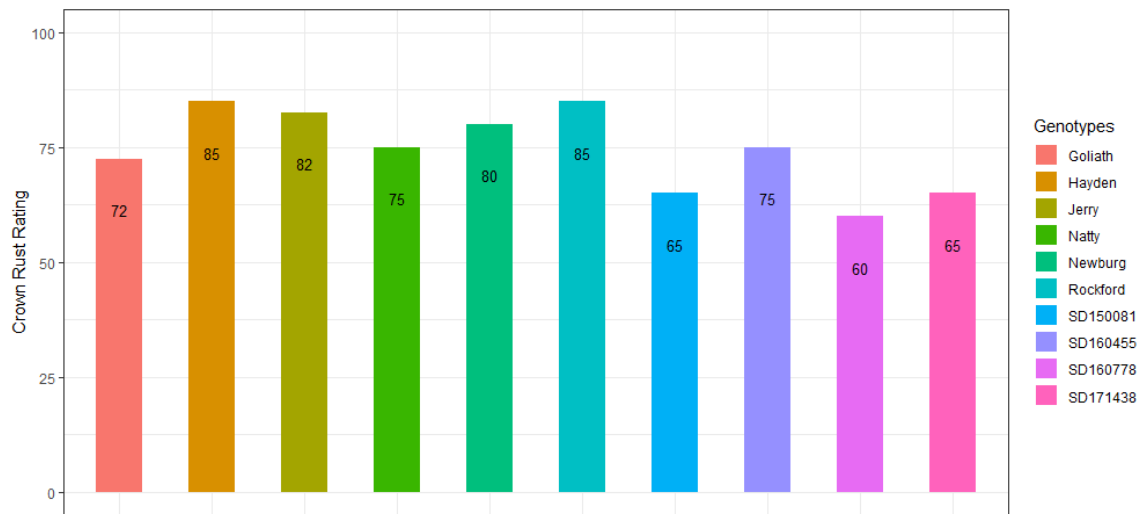


Figure 9: Boxplot representing the distribution of crown rust severity for 35 oat genotypes evaluated at three locations in 2019.

Location: Beresford



Location: Volga



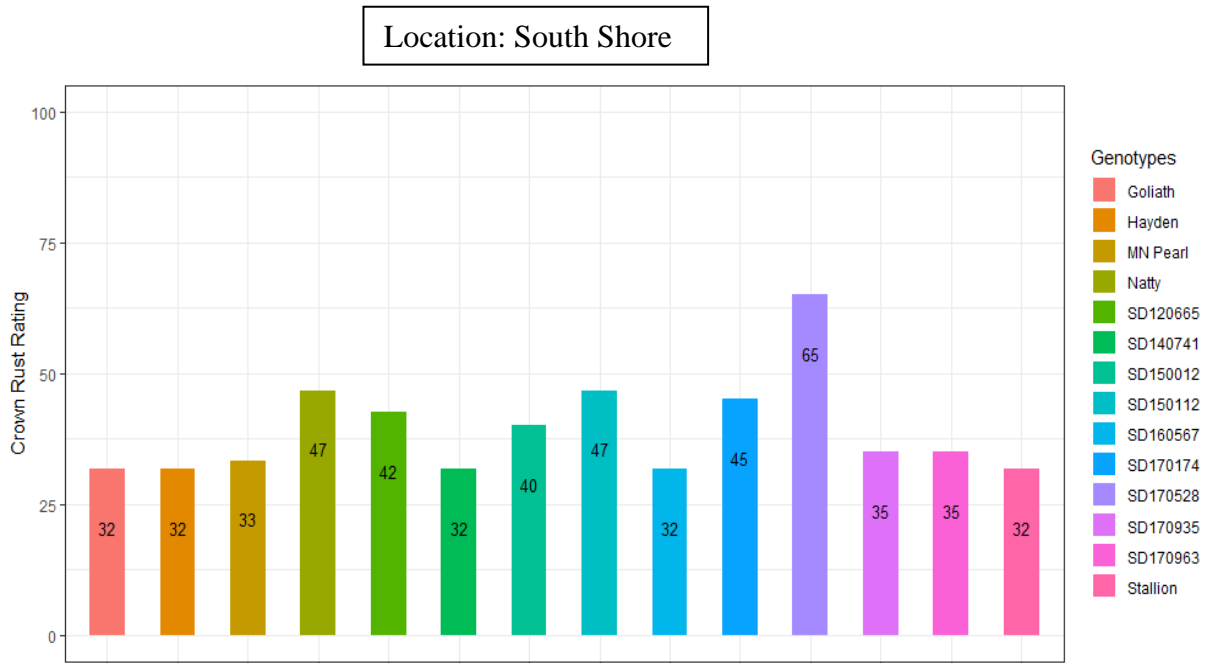
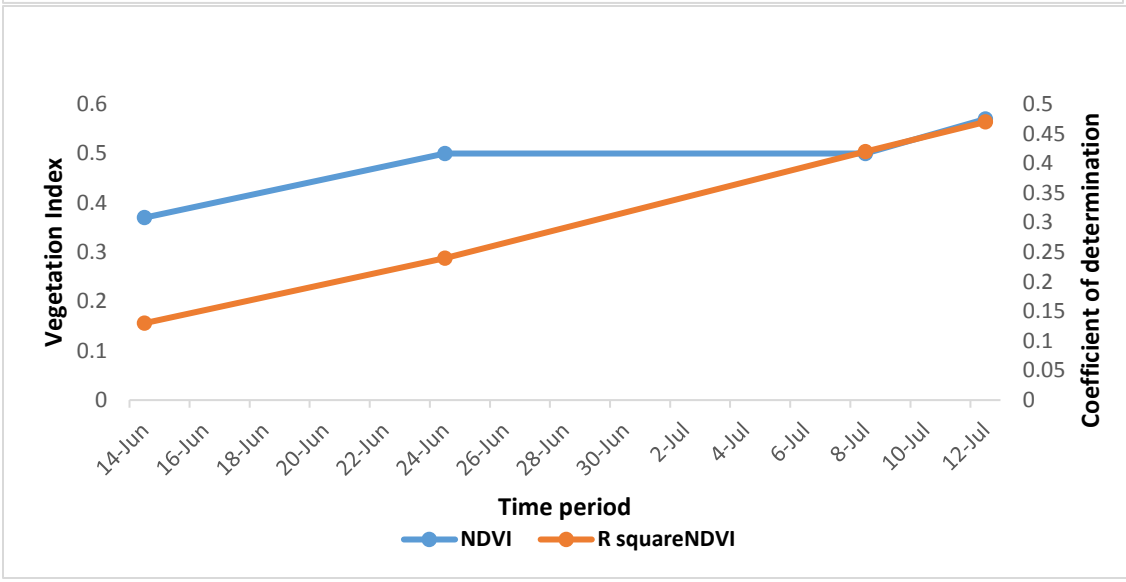
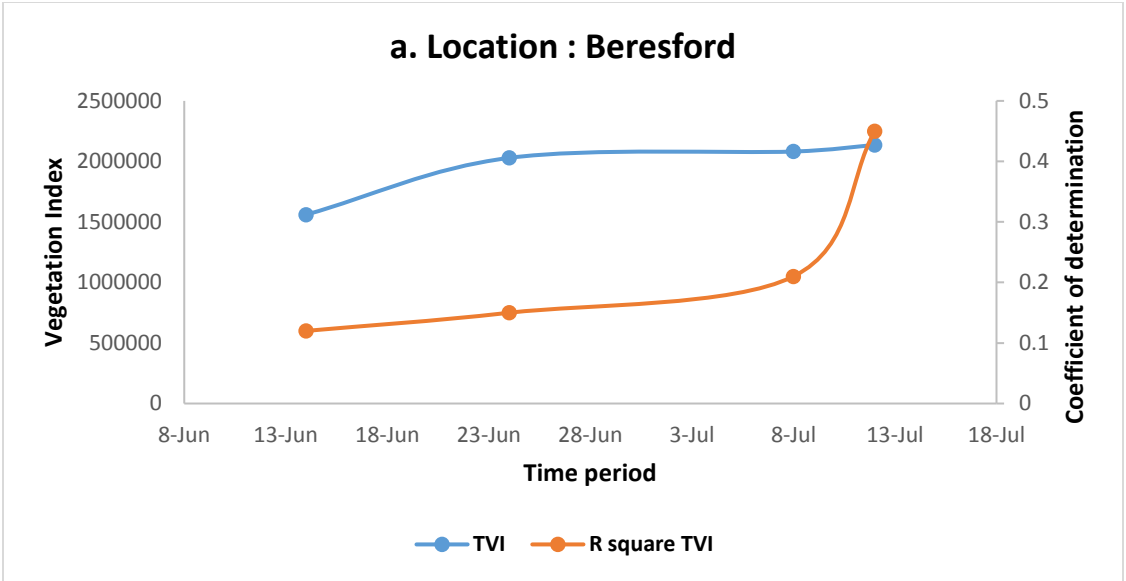
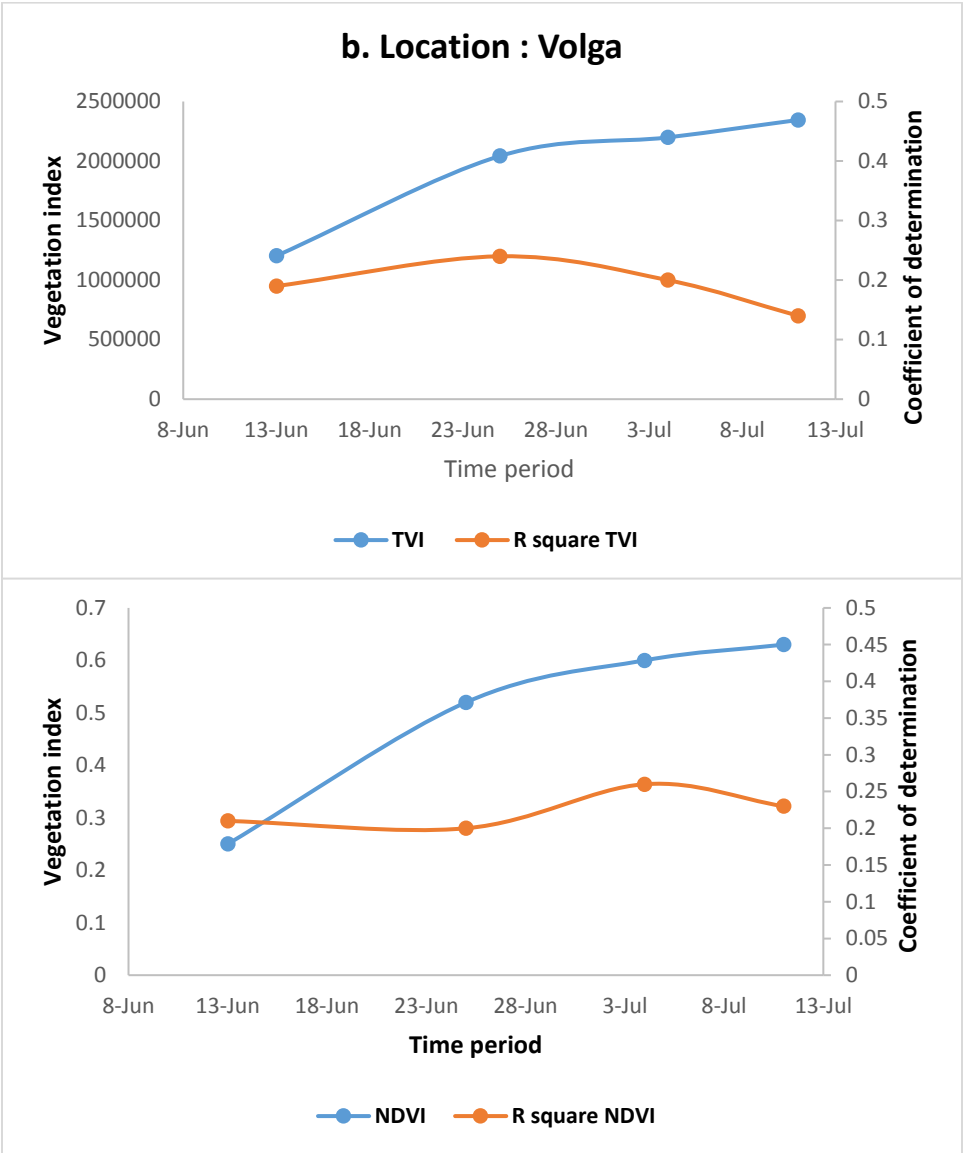


Figure 10: Bar plot representing the distribution of 14 genotypes selected based on highest crown rust severity rate in 2019.





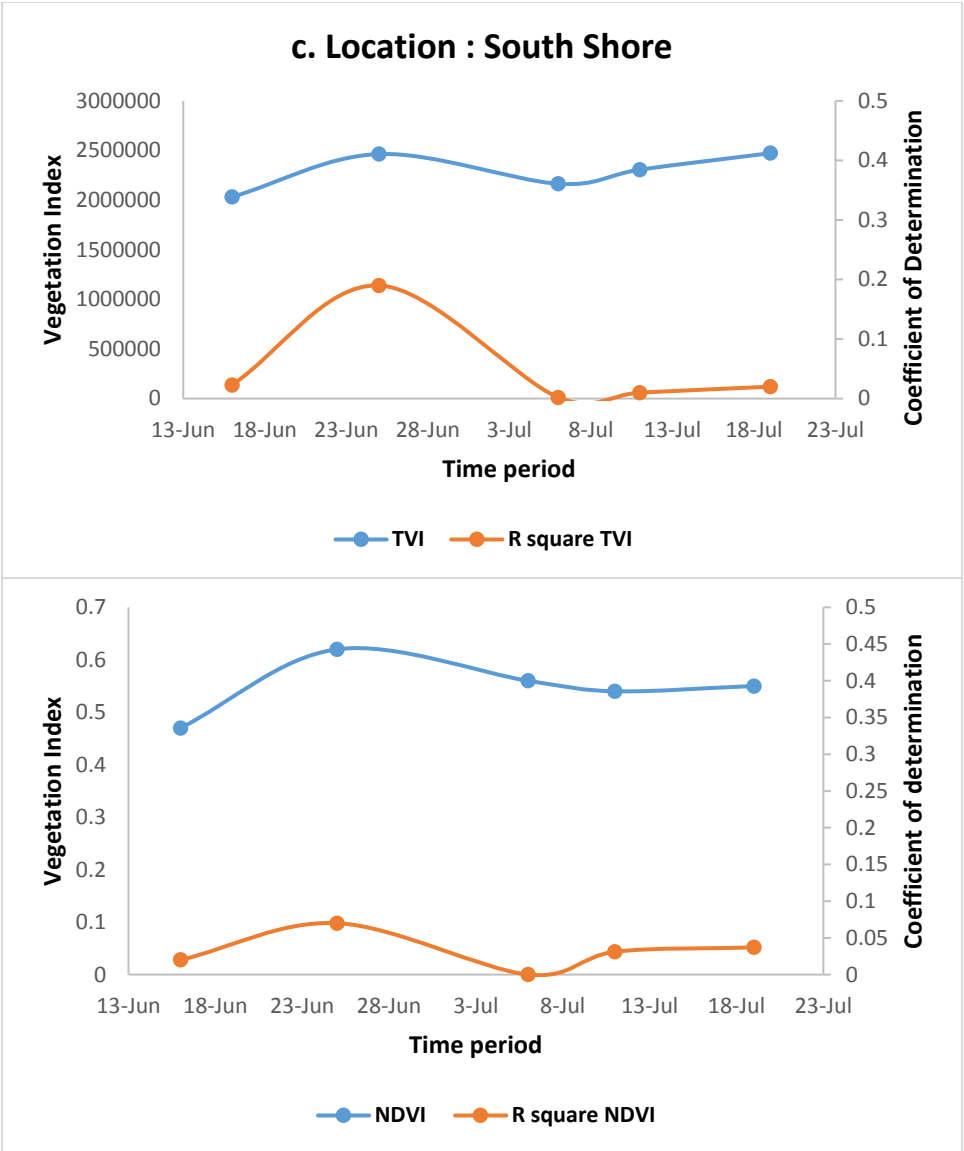
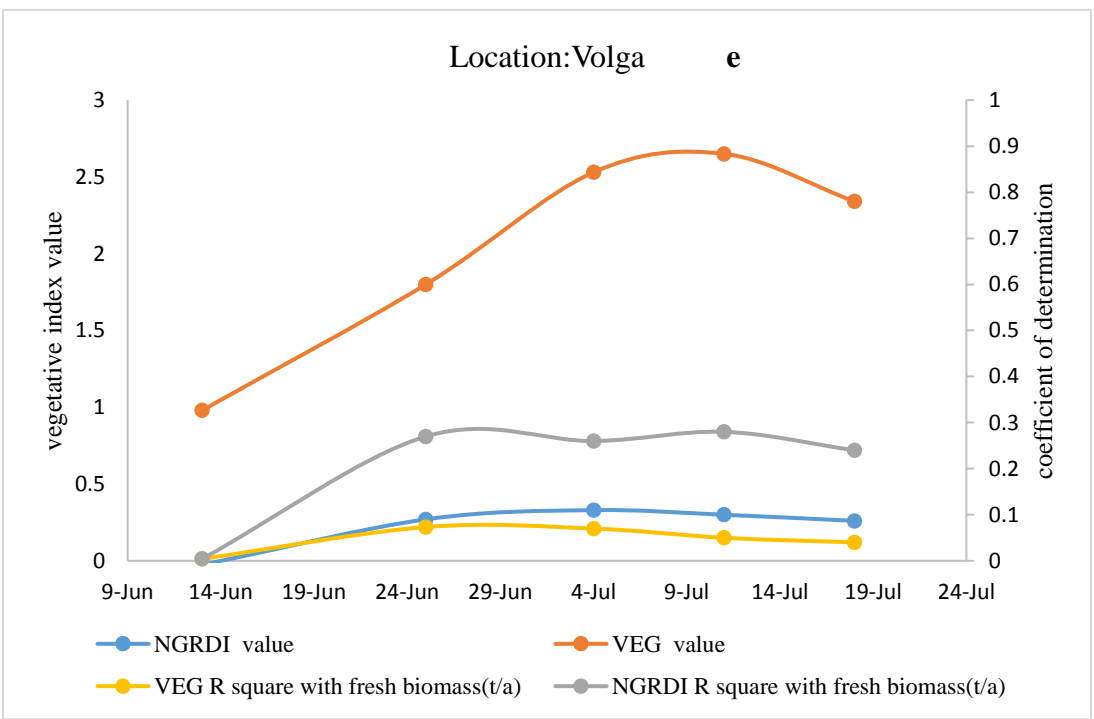
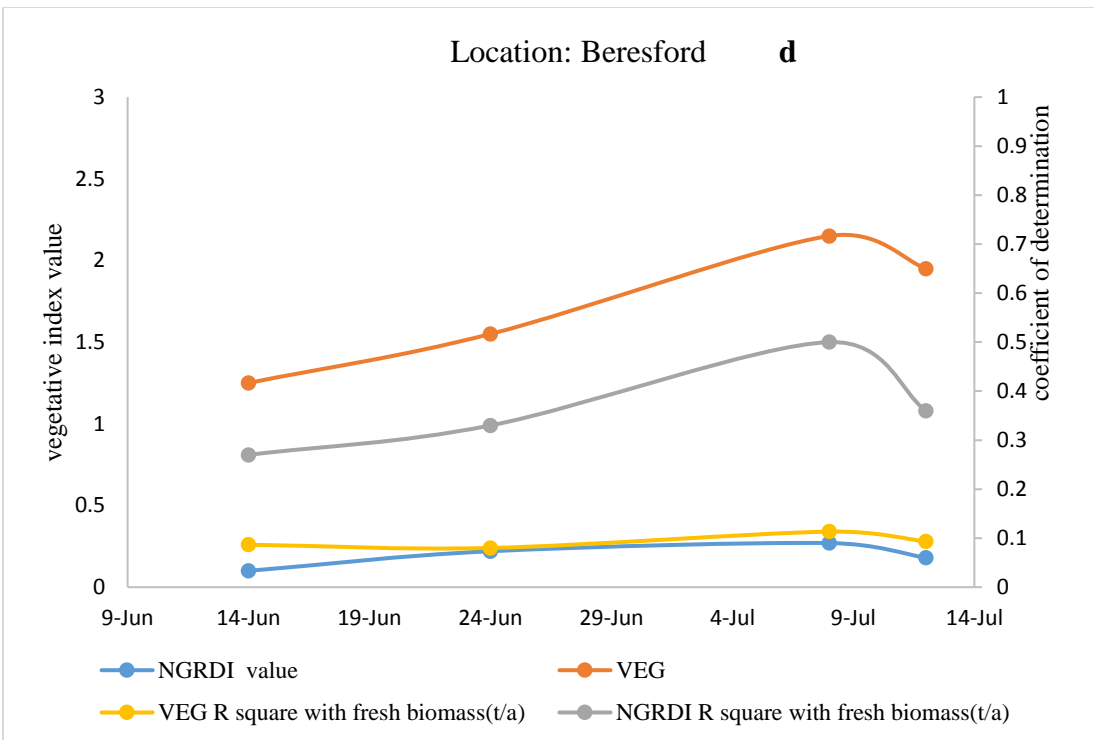


Figure 11: Average NDVI and TVI values derived from imagery collected with a UAV equipped with a Micasense sensor at various dates during the 2019 growing season and coefficient of determination value (R-square) for fresh biomass prediction for 35 oat genotypes grown in Beresford (a), Volga (b) and South Shore (c).



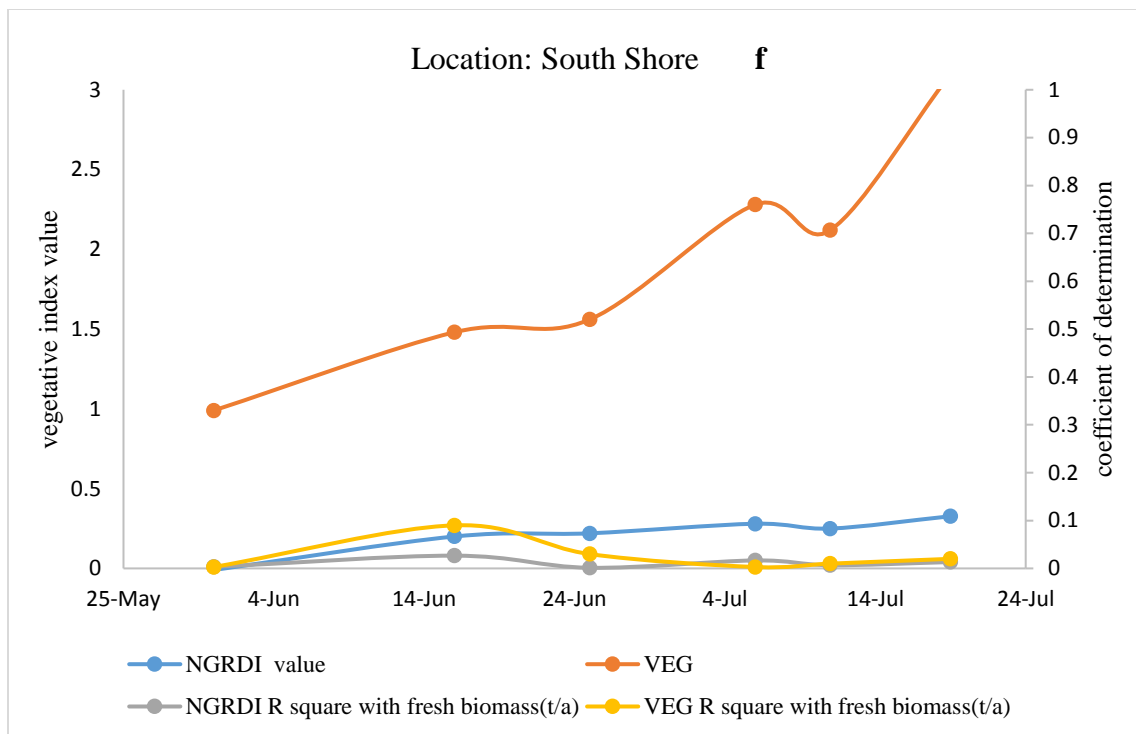
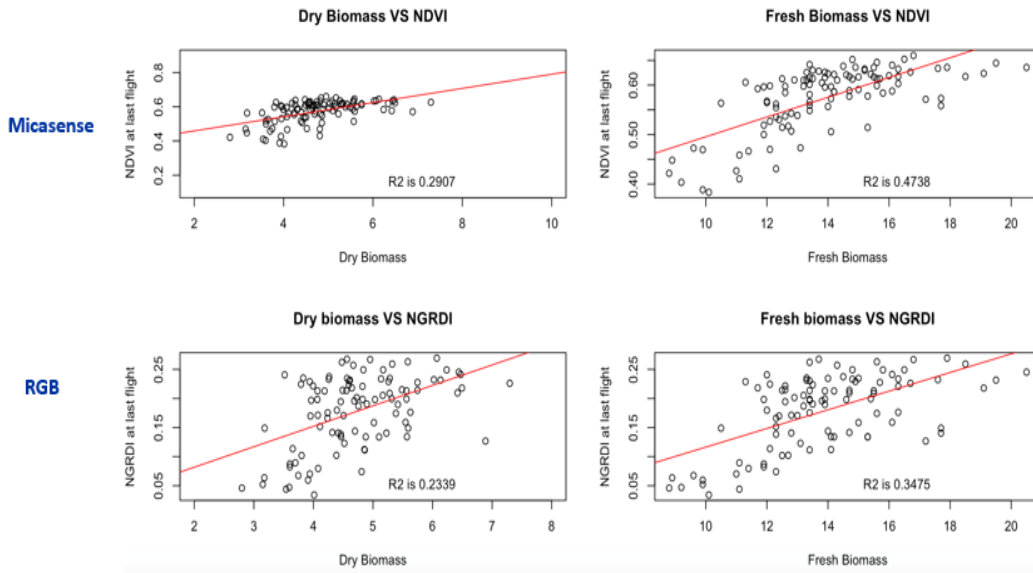
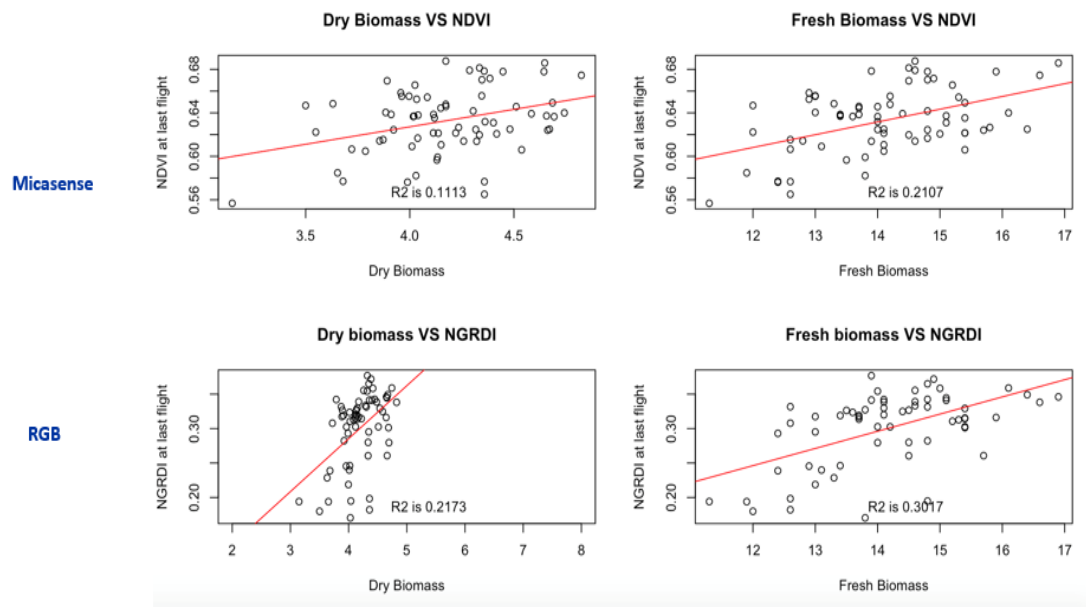


Figure 12: Average NGRDI and VEG values derived from imagery collected with a UAV equipped with a RGB sensor at various dates during the 2019 growing season and coefficient of determination value (R-square) for fresh biomass prediction for 35 oat genotypes grown in Beresford (d), Volga (e) and South Shore (f)

a. Beresford



b. Volga



c. South Shore

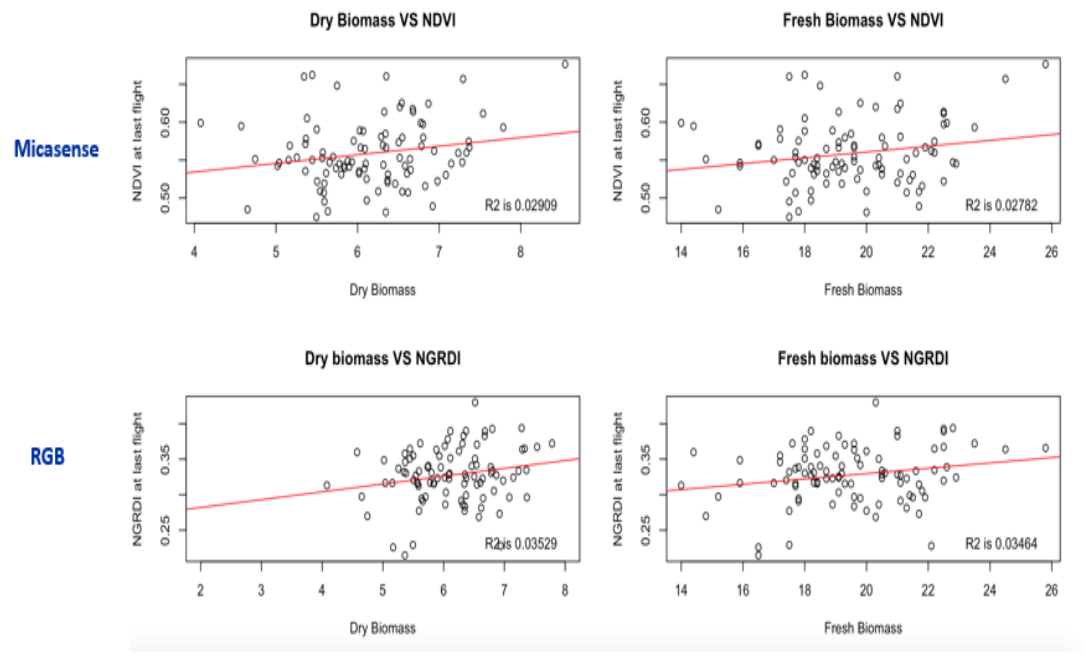


Figure 13 a, b, c: Scatterplots of VI (derived from the last flight) by dry and fresh biomass for each sensor types and each location in 2019.

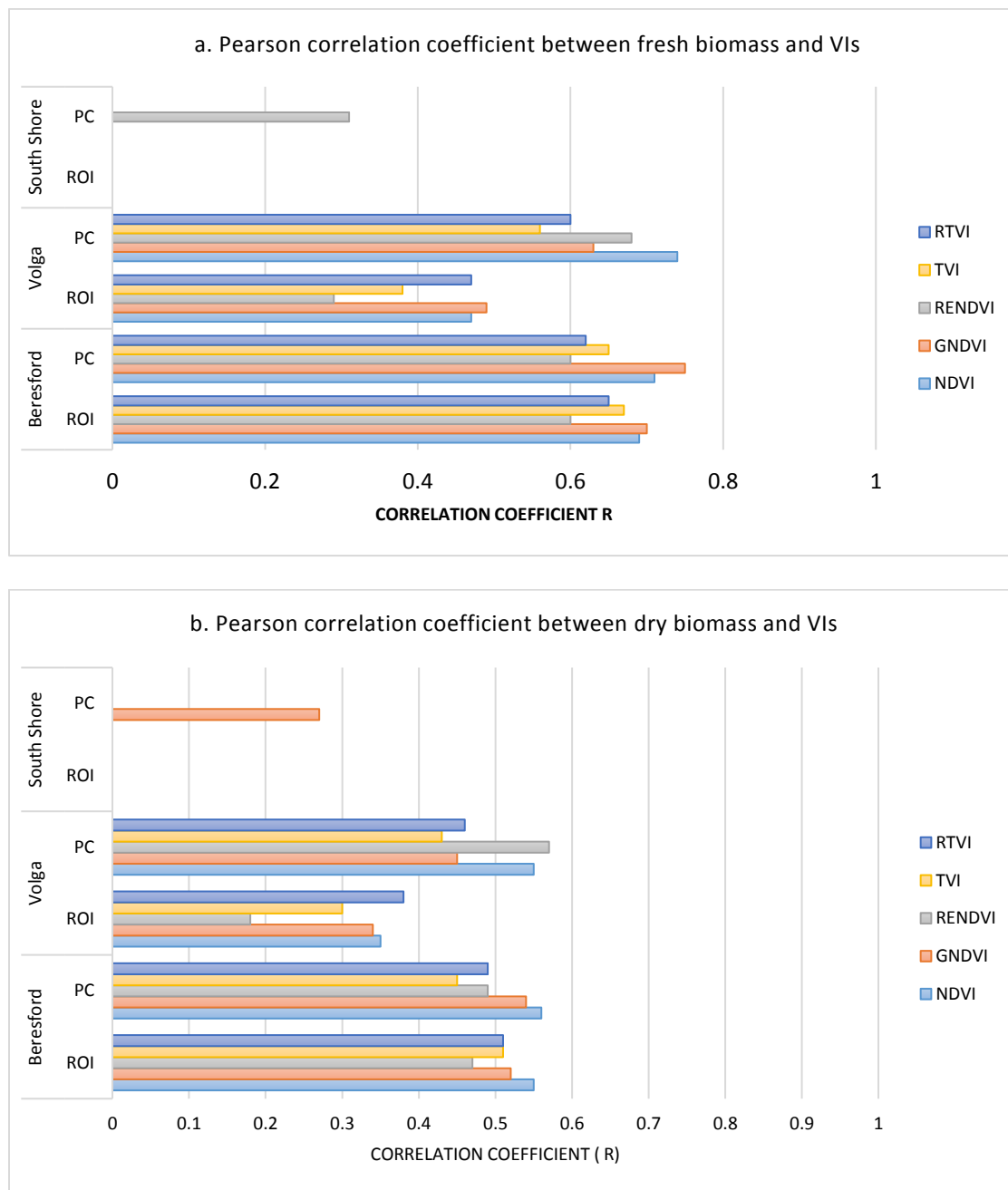


Figure 14: Comparison of pixel under ROI (ROI) and Pixel Classification method (PC) considering correlation coefficient for last flight derived VIs from Micasense with fresh biomass (a) and dry biomass (b).

TABLES


Table 1: Planting and harvesting dates of the oat forage trials conducted at three locations in 2018 and four locations in 2019.

Year	Operation	Beresford	Volga	South Shore	Pierre
2018	Planting	4/27	4/30	5/15	-
	Harvest	7/3	7/2	7/15	-
2019	Planting	4/26	5/14	5/7	4/9
	Harvest	7/11	7/18	7/19	7/2

Table 2: Sensors specification.

Year	Sensor	Platform (UAV)	Sensor resolution (MP)	Focal length	Center Wavelength	Wavelength bandwidth
2018 (Multispectral)	Slantrange	DJI Matrice 600	12 MP	0.012m	NIR (850nm) Green (550 nm) Red (650 nm) Red edge (710 nm)	NIR(50nm) Green (40 nm) Red (40 nm) Red edge (20 nm)
2019 (Multispectral)	Micasense	DJI Matrice 600	3.2 MP per EO band at 400 ft AGL	0.008m (multispectral) 0.0017m (thermal)	Blue (475 nm) Green (560 nm) Red (668 nm) Red edge (717 nm) Near-IR (840 nm)	Blue (20 nm) Green (20 nm) Red (10 nm) Red edge (10 nm) Near-IR (40 nm)
2019 (RGB)	DJI 4K camera (1" CMOS)	DJI Phantom 4 Pro	20.1 MP	0.0027 m	Blue Green Red	Blue Green Red

Table 3. Flight dates and sensors used for collecting imagery of the oat forage trials with an unmanned aerial vehicle at each testing site in 2018 and 2019.



Sensor types	Location	Flight dates
Slant range	Beresford	June 15, June 22, June 26
	Volga	June 12, June 21
	Southshore	June 20, June 12
Mica sense	Beresford	June 14, June 24, July 8, July 12
	Volga	June 13, June 25, July 4, July 11
	Southshore	June 16, June 25, July 6, July 11, July 18, July 19
	Pierre	July 2
RGB (Visual)	Beresford	June 14, July 1, July 8, July 12
	Volga	June 13, June 25, July 4, July 11, July 18
	Southshore	May 31, June 16, June 25, July 6, July 11, July 19

Table 4. Vegetation indices derived from multispectral sensors

Vegetative Index	Source	Abbreviation	Mathematical formula from SR
Normalized Differential Vegetation Index	(Rouse et al. 1974)	NDVI	$(\text{NIR}-\text{R})/(\text{NIR}+\text{R})$
Green Normalized Differential Vegetation Index	(Moges et al. (2004))	GNDVI	$(\text{NIR}-\text{G})/(\text{NIR}+\text{G})$
Triangular Vegetation index	(Broge and Leblanc (2000))	TVI	$0.5*(120*(\text{NIR}-\text{G})-200*(\text{R}-\text{G}))$
Normalized Differential Red edge Index	(Gitelson and Merzlyak, 1994)	RENDVI	$(\text{NIR}-\text{RE})/(\text{NIR}+\text{RE})$
Red edge Triangular Vegetation Index	(Pf Chen, 2010)	RTVI	$100*(\text{NIR}-\text{RE})-10*(\text{NIR}-\text{G})$

Table 5: Vegetation indices derived from visual sensors

Vegetative index	Source	Abbreviation	Mathematical formula from spectral reflectance
Normalized Green Red Differential Index	(Gitelson et al. 2002)	NGRDI	$(R-G)/(R+G)$
Excess green	(Woebbecke et al 1995)	EXG	$2G-R-B$
Excess green minus excess red	(Camargo Neto , 2014)	EXGR	$EXG-1.4R-G$
Vegetetiven	(Hague,Tillett and Wheeler, 2006)	VEG	G/R^aB^{1-a} with $a = 0.667$
Combination	(Guijarro et al., 2011)	COM	$0.25 EXG+0.3 EXGR+0.33 CIVE+0.12 VEG$

Table 6: The Pearson correlation coefficient value derived from dry and fresh biomass versus independent variables for 2018

Location	Biomass	Chlorophyll content	Leaf to stem ratio	Heading date	Crown rust severity	Plant height	Forage rating
Beresford	fresh	0.17	0.05	0.41	NA	NA	0.41
	dry	0.26	0.11	0.05	NA	NA	0.05
Volga	fresh	0.19	0	0.47	-0.1	0.18	NA
	dry	0.16	0.03	0.03	-0.07	0.1	NA
South Shore	fresh	0.09	0.4	0.33	0.06	0.14	0.27
	dry	0.12	0.28	0.06	0.06	0.10	0.15

Highlighted numbers in the table are significant at 95% CI.

Table 7: The Pearson correlation coefficient value derived from dry and fresh biomass versus independent variables for 2019

Location	Biomass	Plant height	Crown rust severity	Heading date	Forage rating
Beresford	fresh	0.44	-0.59	0.19	NA
	dry	0.38	-0.48	0.16	NA
Volga	fresh	0.35	-0.4	0.11	NA
	dry	0.15	-0.32	-0.001	NA
South shore	fresh	0.29	0.06	0.03	-0.03
	dry	0.24	0.09	0.01	-0.04
Pierre	fresh	0.38	NA	0.53	NA
	dry	0.28	NA	0.08	NA

Highlighted numbers in the table are significant at 95% CI

Table 8: The table representing the range, mean and heritability of forage and agronomic traits in different location for year 2018.

	Volga			Beresford			South Shore		
	Range	Mean	Heritability	Range	Mean	Heritability	Range	Mean	Heritability
Fresh biomass	3.6	6.92	0.35	10	16.5	0.43	10.5	17.55	0.5
Dry biomass	1	2.46	0.03	2.1	4.09	0.29	2.8	5.24	0.24
Heading date (HD)	9	167.3	0.88	15	169.9	0.83	12	184.1	0.21
Chlorophyll	20.12	50.68	0.17	14.28	53.09	0.42	13.22	46.4	0.34
Leaf to stem ratio	0.43	0.46	0.25	NA	NA	NA	0.19	0.33	0.41
Plant Height	23	35.29	0.40	NA	NA	NA	13	47.28	0.72
Crown Rust Rate	55	15.19	0.83	NA	NA	NA	85	44.43	0.51

Table 9: The table representing the range, mean and heritability of forage and agronomic traits in different location for year 2019.

	Volga			Beresford			South Shore			Pierre		
	Range	Mean	Heritability	Range	Mean	Heritability	Range	Mean	Heritability	Range	Mean	Heritability
Fresh biomass	5.6	14.1	0.44	11.7	13.89	0.44	11.8	19.49	0.16	7.4	17.74	0.62
Dry biomass	1.67	4.17	0.34	4.5	4.75	0.55	4.46	6.15	0.29	2.02	4.89	0.5
Heading date	8	187	0.79	9	179.7	0.86	9	185.6	0.57	9	173.3	0.89
Plant Height	13	41.1	0.52	16	43.6	0.64	19	47.25	0.48	13	40.99	0.77
Crown rust score	75	43.5	0.9	80	50.78	0.72	65	28.9	0.85	NA	NA	NA
Ligule height	15	31.8	0.89	15	31.55	0.63	13	35.09	0.57	16	29.8	0.35

Table 10: Pearson correlation coefficient between VIs from CropScan sensor and fresh and dry biomass for 35 oat genotypes evaluated at three locations in 2019.

Biomass Type	Fresh Biomass					Dry Biomass				
	NDVI	GNDVI	RENDVI	TVI	RTVI	NDVI	GNDVI	RENDVI	TVI	RTVI
Beresford	0.78	0.6	0.65	0.65	0.71	0.63	0.48	0.55	0.57	0.62
Volga	0.56	0.46	0.54	0.49	0.55	0.48	0.41	0.4	0.38	0.43
South Shore	0.02	0.01	-0.05	-0.17	-0.16	0	0	-0.05	-0.17	-0.16

Note: Highlighted numbers in the table are significant at 95% CI.

Abbreviated forms;

NDVI: Normalized Differential Vegetation Index

GNDVI: Green Normalized Vegetation Differential Index

RENDVI: Red Edge Normalized Vegetation Differential Index

TVI: Triangular Vegetation Index

RTVI: Red edge Triangular Vegetation Index

Table 11: Pearson correlation coefficient between VIs derived from the Slantrange sensor and fresh and dry biomass for 35 oat genotypes evaluated at three locations in 2018.

Biomass Type	Fresh Biomass				Dry Biomass			
	NDVI	GNDVI	RENDVI	TVI	NDVI	GNDVI	RENDVI	TVI
Beresford								
15-Jun	0.38	0.49	0.37	0.14	0.43	0.36	0.43	0.22
22-Jun	0.3	0.31	0.34	0.035	0.28	0.1	0.23	0.06
26-Jun	0.18	0.21	0.1	0.31	0.14	0.17	0.12	0.09
Volga								
12-Jun	0.45	0.41	0.2	0.1	0.48	0.56	0.27	0.12
21-Jun	0.55	0.5	0.32	0.48	0.46	0.48	0.37	0.43
South Shore								
20-Jun	0.07	0.09	0.08	0.12	0	0	0.07	0.06
12-Jun	-0.04	0	0.08	0.08	0	0	0	0.08

Note: Highlighted numbers in the table are significant at 95% CI.

Abbreviated forms;

NDVI: Normalized Differential Vegetation Index

GNDVI: Green Normalized Vegetation Differential Index

RENDVI: Red Edge Normalized Vegetation Differential Index

TVI: Triangular Vegetation Index

RTVI: Red edge Triangular Vegetation Index

Table 12: Pearson correlation coefficient between VIs derived from Micasense and RGB sensor and fresh/dry biomass for 35 different oat genotypes in Volga 2019.

Biomass										
Type	Fresh Biomass					Dry Biomass				
Flights	NDVI	GNDVI	RENDVI	TVI	RTVI	NDVI	GNDVI	RENDVI	TVI	RTVI
13-Jun	0.46	0.38	0.38	0.44	0.43	0.36	0.33	0.23	0.35	0.47
25-Jun	0.46	0.32	0.47	0.55	0.41	0.29	0.21	0.29	0.39	0.29
4-Jul	0.52	0.43	0.36	0.44	0.47	0.37	0.33	0.17	0.35	0.42
11-Jul	0.47	0.49	0.29	0.38	0.47	0.35	0.34	0.18	0.3	0.38
	NGRDI	EXG	EXGRR	VEG	COM	NGRDI	EXG	EXGRR	VEG	COM
13-Jun	0.07	0.15	0.32	0.12	0.31	0.02	0.1	0.17	0.04	0.17
25-Jun	0.26	0.04	0.18	0.15	0.17	0.07	0.05	0.1	0.02	0.06
4-Jul	0.52	0.3	0.21	0.47	0.26	0.46	0.2	0.21	0.47	0.25
11-Jul	0.54	0.05	0.35	0.39	0.35	0.33	0.03	0.2	0.26	0.18
18-Jul	0.49	0.11	0.34	0.35	0.34	0.44	0.03	0.38	0.36	0.37

Note: Highlighted numbers in the table are significant at 95% CI.

Abbreviated forms;

NDVI: Normalized Differential Vegetation Index

GNDVI: Green Normalized Vegetation Differential Index

RENDVI: Red Edge Normalized Vegetation Differential Index

TVI: Triangular Vegetation Index

RTVI: Red edge Triangular Vegetation Index

NGRDI: Normalized Green Red Differential Index

EXG: Excess Green

EXGR: Excess Green minus Red

VEG: Vegetation

COM: Combination

Table 13: Pearson Correlation coefficient VIs derived from Micasense and RGB sensor and fresh/dry biomass for 35 different oat genotypes in Beresford 2019.

Biomass Type	Fresh Biomass					Dry Biomass				
	NDVI	GNDVI	RENDVI	TVI	RTVI	NDVI	GNDVI	RENDVI	TVI	RTVI
14-Jun	0.37	0.27	0.22	0.35	0.38	0.23	0.21	0.25	0.18	0.32
24-Jun	0.49	0.44	0.33	0.46	0.4	0.35	0.29	0.19	0.32	0.22
8-Jul	0.65	0.55	0.5	0.4	0.6	0.51	0.44	0.4	0.3	0.47
12-Jul	0.69	0.7	0.6	0.67	0.65	0.55	0.52	0.47	0.51	0.51
	NGRDI	EXG	EXGRR	VEG	COM	NGRDI	EXG	EXGRR	VEG	COM
14-Jun	0.52	0.43	0.49	0.5	0.48	0.35	0.3	0.34	0.33	0.33
24-Jun	0.58	0.22	0.33	0.49	0.36	0.46	0.16	0.3	0.4	0.32
8-Jul	0.71	0.15	0.63	0.59	0.64	0.55	0.15	0.46	0.43	0.47
12-Jul	0.61	0.4	0.53	0.53	0.56	0.49	0.39	0.42	0.45	0.45

Note: Highlighted numbers in the table are significant at 95% CI.

Abbreviated forms;

NDVI: Normalized Differential Vegetation Index

GNDVI: Green Normalized Vegetation Differential Index

RENDVI: Red Edge Normalized Vegetation Differential Index

TVI: Triangular Vegetation Index

RTVI: Red edge Triangular Vegetation Index

NGRDI: Normalized Green Red Differential Index

EXG: Excess Green

EXGR: Excess Green minus Red

VEG: Vegetation

COM: Combination

Table 14: Pearson correlation coefficient VIs derived from Micasense and RGB sensor and fresh/dry biomass for 35 different oat genotypes in South Shore 2019.

Biomass Type	Fresh Biomass					Dry Biomass				
	NDVI	GNDVI	TVI	RTVI	RENDVI	NDVI	GNDVI	TVI	RTVI	RENDVI
16-Jun	-0.11	-0.16	0.15	0.07	0	-0.14	-0.16	0.1	0.09	0
25-Jun	0.03	-0.4	0.41	-0.14	-0.31	-0.08	-0.37	0.35	-0.14	-0.29
6-Jul	-0.07	-0.08	0.05	0.03	-0.09	-0.09	-0.1	0.03	-0.05	-0.09
11-Jul	-0.18	0.17	-0.13	0.19	0.22	-0.12	0.23	-0.01	0.25	0.27
18-Jul	0.19	0.16	0.1	0.19	0.19	0.18	0.15	0.11	0.16	0.15
19-Jul	0.2	0.27	0.14	0.19	0.18	0.2	0.27	0.18	0.15	0.14
	NGRDI	EXG	EXGR	VEG	COM	NGRDI	EXG	EXGR	VEG	COM
31-May	0.1	0.02	-0.006	0.03	-0.06	0.09	0.016	-0.03	0.02	-0.031
16-Jun	0.06	0.33	0.35	0.14	0.093	0.04	0.25	0.2	0.075	0.118
25-Jun	-0.03	0.3	0.21	0.026	-0.18	0.06	0.22	0.19	0	-0.17
6-Jul	0.22	0.007	0.048	-0.02	0.06	0.14	0.08	0.003	-0.4	0.003
11-Jul	0.14	0.011	-0.08	-0.1	-0.1	0.18	-0.03	-0.02	-0.08	-0.04
19-Jul	0.21	0.023	0.168	0.124	0.166	0.21	0.042	0.22	0.2	0.23

Note: Highlighted numbers in the table are significant at 95% CI.

Abbreviated forms;

NDVI: Normalized Differential Vegetation Index

GNDVI: Green Normalized Vegetation Differential Index

RENDVI: Red Edge Normalized Vegetation Differential Index

TVI: Triangular Vegetation Index

RTVI: Red edge Triangular Vegetation Index

NGRDI: Normalized Green Red Differential Index

EXG: Excess Green

EXGR: Excess Green minus Red

VEG: Vegetation

COM: Combination

Table 15: Pearson correlation coefficient between VIs from UAV (sensor Mica sense) and VIs from Crop scan in all location for 2019.

	Beresford	Volga	South Shore
NDVI	0.78	0.37	0.21
GNDVI	0.67	0.29	0.36
RENDVI	0.6	0.45	0.41
TVI	0.62	0.63	0.27
RTVI	0.65	0.69	0.14

Note: Highlighted numbers in the table are significant at 95% CI.

Abbreviated forms;

NDVI: Normalized Differential Vegetation Index

GNDVI: Green Normalized Vegetation Differential Index

RENDVI: Red Edge Normalized Vegetation Differential Index

TVI: Triangular Vegetation Index

RTVI: Red edge Triangular Vegetation Index

Table 16: Prediction models for dry biomass harvested from 35 different oat genotypes using VI derived from the Slantrange sensor and agronomic characteristics as predictor variables for 2018. All the model selected on 95% confidence interval and the models not significant are represented as NS

Biomass Type: Dry	Sensor Type: Slantrange		
	Variables	R-square	RMSE
Vegetation Indexes only			
Volga	June 12 (GNDVI), June 21 (TVI)	0.32	0.16
Beresford	June 15 (NDVI) June 22(GNDVI)	0.24	0.36
South Shore	-	NS	NS
Agronomic characteristics only			
Volga	Chlorophyll	0.03	0.2
Beresford	Chlorophyll	0.05	0.4
South Shore	HT, Leaf to Stem ratio	0.09	0.48
Combination of VI and agronomic characteristics			
Volga	Chlorophyll, June 12 (GNDVI), June 21 (TVI)	0.35	0.16
Beresford	Chlorophyll, June 15 (NDVI) June 22(GNDVI)	0.3	0.35
South Shore	HT, Leaf to Stem ratio	0.09	0.48

Note: Highlighted numbers in the table are significant at 95% CI.

Abbreviated forms;

NDVI: Normalized Differential Vegetation Index

GNDVI: Green Normalized Vegetation Differential Index

RENDVI: Red Edge Normalized Vegetation Differential Index

TVI: Triangular Vegetation Index

RTVI: Red edge Triangular Vegetation Index

HT: Plant height

NS: Non-significant

Table 17: Prediction models for fresh biomass harvested from 35 different oat genotypes using VI derived from the Slantrange sensor and agronomic characteristics as predictor variables for 2018. All the model selected on 95% confidence interval and the models not significant are represented as NS

Biomass Type: Fresh	Sensor Type: Slantrange		
	Variables	R-square	RMSE
Vegetation Indexes only			
Volga	June 12 (GNDVI), June 21 (NDVI)	0.36	0.57
Beresford	, June 15 (NDVI) June 22(GNDVI), June 26 (TVI)	0.35	1.44
South Shore	-	NS	NS
Agronomic characteristics only			
Volga	HD, Chlorophyll	0.28	0.61
Beresford	HD, Chlorophyll	0.14	1.96
South Shore	HD, HT, Leaf to Stem ratio	0.23	1.85
Combination of VI and agronomic characteristics			
Volga	Chlorophyll, HD, Leaf to Stem ratio, June 12 (GNDVI) June 21 (NDVI)	0.5	0.51
Beresford	HD, Chlorophyll, June 15 (NDVI) June 22(GNDVI)	0.42	1.37
South Shore	HD, HT, Leaf to Stem ratio	0.23	1.85

Note: Highlighted numbers in the table are significant at 95% CI.

Abbreviated forms;

NDVI: Normalized Differential Vegetation Index

GNDVI: Green Normalized Vegetation Differential Index

RENDVI: Red Edge Normalized Vegetation Differential Index

TVI: Triangular Vegetation Index

RTVI: Red edge Triangular Vegetation Index

HT: Plant height

NS: Nonsignificant

Table 18: Prediction models for dry biomass harvested from 35 different oat genotypes using VI derived from the Micasense and RGB sensor and agronomic characteristics as predictor variables for 2019. All the model selected on 95% confidence interval and the models not significant are represented as NS

Biomass Type :	Micasense			RGB		
	Variables	R-square	RMSE	Variables	R-square	RMSE
Dry						
Vegetation Indexes only						
Volga	June 13 (GNDVLRTV), June 25 (GNDVJJuly 4(RTV), July 11 (NDVJGNDV))	0.56	0.22	June 25(EXGR, NGRD), July 18 (NGRD)	0.5	0.24
Beresford	June 14 (RTVJGNDV), July 8 (RENDVJGNDV), July 12 (NDV)	0.46	0.64	June 14(NGRD), July 8 (NGRD), EXGR	0.4	0.68
South Shore	June 25(GNDV), July 19(GNDVJRENDV)	0.21	0.68	June 16(COM), July 11 (NGRD), VEG, ENG	0.17	0.68
Pierre	July 2(NDVJRENDV)	0.12	0.33	-	-	-
Agronomic characteristics only						
Volga	CR	0.1	0.3	CR	0.1	0.3
Beresford	HT, CR	0.36	0.7	HT, CR	0.36	0.7
South Shore	-	NS	NS	-	-	-
Pierre	HT, HT_ligule	0.12	0.32	HT, HT_ligule	0.12	0.32
Combination of VI and agronomic characteristics						
Volga	June 13 (GNDVLRTV), June 25 (GNDV), July 4(RTV), July 11 (NDVJGNDV)	0.58	0.22	June 25(EXGR, VEG), July 18 (NGRD)	0.54	0.22
Beresford	June 14 (RTV), July 8 (TV), July 12(NDV), HT	0.54	0.62	HT, CR, NGRD	0.49	0.65
South Shore	June 25(GNDV), July 19(GNDVJRENDV), CR	0.22	0.68	June 16(ENG), July 11 (NGRD), VEG, CR	0.12	0.71
Pierre	July 2(NDV), HT, HT_ligule	0.17	0.31	-	-	-

Note: Highlighted numbers in the table are significant at 95% CI.

Abbreviated forms:

NDVI: Normalized Differential Vegetation Index

GNDVI: Green Normalized Vegetation Differential Index

RENDVI: Red Edge Normalized Vegetation Differential Index

TVI: Triangular Vegetation Index

RTVI: Red edge Triangular Vegetation Index

NGRDI: Normalized Green Red Differential Index

EXG: Excess Green

EXGR: Excess Green minus Red

VEG: Vegetation

COM: Combination

HT: Plant Height

CR: Crown Rust

HT_ligule: Plant height ligule

Table 19: Prediction models for fresh biomass harvested from 35 different oat genotypes using VI derived from the Micasense and RGB sensor and agronomic characteristics as predictor variables for 2019. All the model selected on 95% confidence interval and the models not significant are represented as NS

Biomass Type : Fresh	Micasense		RGB	
	Variables	R-squarr, RMSE	Variables	R-squarr, RMSE
Vegetation Indexes only				
Volga	June 13 (RTVI), June 25 (TVI), July 4 (NDVI), July 14 (RTVI), July 8 (GNDVI), July 12 (TVI), July 16 (TVI), June 25 (GNDVI), July 19 (GNDVI), July 2 (NDVI), July 19 (GNDVI)	0.52 0.85 0.73 1.22 0.19 1.99 0.4 1.22	June 25 (NGRD), EXGR, July 11 (NGRD)	0.72 0.63 0.64 1.42 0.13 2.05
Beresford				
South Shore				
Pierre				
Agronomic characteristics only				
Volga	HT, CR	0.28 1.03	HT, CR	0.28 1.03
Beresford	HT, CR	0.55 1.56	HT, CR	0.55 1.56
South Shore	—	NS NS	—	—
Pierre	HD, HT, HT_ligule	0.44 1.14	HD, HT, HT_ligule	0.44 1.14
of V and agronomic characteristics				
Volga	June 13 (RENDVI), June 25 (TVI), July 4 (NDVI), CR	0.6 0.79	June 25 (NGRD), EXGR, July 11 (NGRD), CR	0.75 0.62
Beresford	June 14 (RTVI), June 24 (RTVI), July 8 (NDREI), July 12 (NDVI), July 19 (GNDVI), CR	0.84 0.98	June 14 (NGRD), July 1 (EXGR), July 8 (NGRD), HT, CR	0.73 1.28
South Shore	June 16 (TVI), June 25 (GNDVI), July 19 (GNDVI), CR	0.2 1.99	June 16 (EXG), July 19 (EXGR), HT	0.16 2.03
Pierre	July 2 (RTVI), HT, HT_ligule, HD	0.51 1.07	—	—

Note: Highlighted numbers in the table are significant at 95% CI.

Abbreviated forms:

NDVI: Normalized Differential Vegetation Index

GNDVI: Green Normalized Vegetation Differential Index

RENDVI: Red Edge Normalized Vegetation Differential Index

TVI: Triangular Vegetation Index

RTVI: Red edge Triangular Vegetation Index

NGRD: Normalized Green Red Differential Index

EXG: Excess Green

EXGR: Excess Green minus Red

VEG: Vegetation

COM: Combination

HT: Plant Height

CR: Crown Rust

HT_ligule: Plant height ligule

Table 20: Pearson correlation between VI derived using the pixel classification method from imagery collected with the Micasense sensor and biomass for 35 oat genotypes in 2019.

Beresford 2019										
Biomass										
Type	Fresh Biomass					Dry Biomass				
	NDVI	GNDVI	RENDVI	TVI	RTVI	NDVI	GNDVI	RENDVI	TVI	RTVI
14-Jun	0.5	0.35	0.34	0.44	0.28	0.34	0.21	0.22	0.3	0.1
24-Jun	0.67	0.52	0.47	0.48	0.58	0.51	0.41	0.35	0.36	0.44
8-Jul	0.65	0.48	0.4	0.33	0.35	0.54	0.35	0.43	0.32	0.28
12-Jul	0.71	0.75	0.6	0.65	0.62	0.56	0.54	0.49	0.45	0.49

Volga 2019										
Biomass										
Type	Fresh Biomass					Dry Biomass				
	NDVI	GNDVI	RENDVI	TVI	RTVI	NDVI	GNDVI	RENDVI	TVI	RTVI
13-Jun	0.28	0.25	0.33	0.24	0.32	0.2	0.22	0.37	0.19	0.37
25-Jun	0.42	0.27	0.22	0.48	0.22	0.2	0.13	0.1	0.24	0.15
4-Jul	0.66	0.52	0.48	0.47	0.37	0.4	0.35	0.32	0.35	0.31
11-Jul	0.74	0.63	0.68	0.56	0.6	0.55	0.45	0.57	0.43	0.46

South Shore 2019										
Biomass										
Type	Fresh Biomass					Dry Biomass				
	NDVI	GNDVI	RENDVI	TVI	RTVI	NDVI	GNDVI	RENDVI	TVI	RTVI
16-Jun	-0.02	-0.19	-0.19	0.17	-0.2	-0.09	-0.18	-0.17	0.1	-0.19
25-Jun	-0.37	-0.4	-0.3	0.44	-0.31	-0.33	-0.42	-0.33	0.35	-0.28
6-Jul	0.12	0.08	0.1	0.17	0.12	0.11	0.07	0.12	0.13	0.07
18-Jul	0.32	0.2	0.31	0.2	0.32	0.14	0.27	0.17	0.18	0.17

Note: Highlighted numbers in the table are significant at 95% CI.

Abbreviated forms;

NDVI: Normalized Differential Vegetation Index

GNDVI: Green Normalized Vegetation Differential Index

RENDVI: Red Edge Normalized Vegetation Differential Index

TVI: Triangular Vegetation Index

RTVI: Red edge Triangular Vegetation Index

Table 21: Prediction models for fresh and dry biomass harvested from 35 different oat genotypes using pixel classification method (for Micasense) derived VIs and agronomic characteristics as predictor variables for 2019. All the model selected on 95% confidence interval and the models not significant are represented as NS

Biomass Type: Dry	Micasense: Pixel classification method		
	Variables	R-square	RMSE
Vegetation Indexes only			
Volga	June 13 (GNDVI, RTVI), July 4 (RTVI, TVI), July 11 (RENDVI)	0.48	0.24
Beresford	June 14 (GNDVI, RENDVI) July 8 (NDVI, RENDVI), July 12(NDVI)	0.64	0.54
South Shore	June 25 (GNDVI, RTVI), July 6 (TVI)	0.25	0.63
Combination of VI and agronomic characteristics			
Volga	CR, June 13 (GNDVI, RTVI), July 4 (RTVI), July 11 (RENDVI, NDVI)	0.52	0.22
Beresford	HT, June 14 (GNDVI, RENDVI) July 8 (NDVI, RENDVI), July 12(NDVI)	0.67	0.52
South Shore	June 25 (GNDVI, RTVI), July 6 (TVI)	0.25	0.63
Biomass Type: Fresh			
Vegetation Indexes only		R-square	RMSE
Volga	June 13 (GNDVI, TVI, RTVI), June 25 (NDVI), July 4(NDVI), July 11(NDVI), July 11(NDVI)	0.74	0.63
Beresford	June 14(RENDVI, TVI), June 24(TVI), July 8 (NDVI, RENDVI) July 12(NDVI)	0.87	0.84
South Shore	June 16(TVI, RTVI), June 25 (NDVI, GNDVI, RTVI), July 6 (TVI)	0.44	1.62
Combination of VI and agronomic characteristics			
Volga	CR, June 13 (GNDVI, TVI, RTVI), June 25 (NDVI), July 11(TVI, RTVI, RENDVI)	0.83	0.54
Beresford	HT, HT_Ligule, June 14(RENDVI), June 24(NDVI, RENDVI), July 8 (NDVI, TVI) July 12(NDVI)	0.9	0.77
South Shore	June 16(TVI, RTVI), June 25 (NDVI, GNDVI, RTVI), July 6 (TVI)	0.44	1.62

Note: Highlighted numbers in the table are significant at 95% CI.

Abbreviated forms;

NDVI: Normalized Differential Vegetation Index

GNDVI: Green Normalized Vegetation Differential Index

RENDVI: Red Edge Normalized Vegetation Differential Index

TVI: Triangular Vegetation Index

RTVI: Red edge Triangular Vegetation Index

HT: Plant height

NS: Nonsignificant

5. References

- Aparicio N., Villegas D., Casadesus J., Araus J.L., Royo C. (2000) Spectral vegetation indices as nondestructive tools for determining durum wheat yield. *Agronomy Journal* 92:83-91.
- Aparicio N., Villegas D., Casadesus J., Araus J.L., Royo C. (2000) Spectral vegetation indices as nondestructive tools for determining durum wheat yield. *Agronomy Journal* 92:83-91.
- Babar M., Van Ginkel M., Reynolds M., Prasad B., Klatt A. (2007) Heritability, correlated response, and indirect selection involving spectral reflectance indices and grain yield in wheat. *Australian Journal of Agricultural Research* 58:432-442.
- Ballesteros R., Ortega J.F., Hernandez D., Moreno M.A. (2018) Onion biomass monitoring using UAV-based RGB imaging. *Precision agriculture* 19:840-857.
- Bellairs S., Turner N., Hick P., Smith R. (1996) Plant and soil influences on estimating biomass of wheat in plant breeding plots using field spectral radiometers. *Australian Journal of Agricultural Research* 47:1017-1034.
- Bendig J., Bolten A., Bareth G. (2013) UAV-based imaging for multi-temporal, very high Resolution Crop Surface Models to monitor Crop Growth Variability Monitoring des Pflanzenwachstums mit Hilfe multitemporaler und hoch auflösender Oberflächenmodelle von Getreidebeständen auf Basis von Bildern aus UAV-Befliegungen. *Photogrammetrie-Fernerkundung-Geoinformation* 2013:551-562.
- Bendig J., Bolten A., Bennertz S., Broscheit J., Eichfuss S., Bareth G. (2014) Estimating biomass of barley using crop surface models (CSMs) derived from UAV-based RGB imaging. *Remote Sensing* 6:10395-10412.
- Brocks S., Bareth G. (2018) Estimating barley biomass with crop surface models from oblique RGB imagery. *Remote Sensing* 10:268.
- Calvaio T., Palmeirim J. (2004) Mapping Mediterranean scrub with satellite imagery: biomass estimation and spectral behaviour. *International Journal of Remote Sensing* 25:3113-3126.
- Chen J., Gu S., Shen M., Tang Y., Matsushita B. (2009) Estimating aboveground biomass of grassland having a high canopy cover: an exploratory analysis of in situ hyperspectral data. *International Journal of Remote Sensing* 30:6497-6517.

- Díaz-Varela R., de la Rosa R., León L., Zarco-Tejada P. (2015) High-resolution airborne UAV imagery to assess olive tree crown parameters using 3D photo reconstruction: application in breeding trials. *Remote Sensing* 7:4213-4232.
- Ferrio J., Villegas D., Zarco J., Aparicio N., Araus J., Royo C. (2005) Assessment of durum wheat yield using visible and near-infrared reflectance spectra of canopies. *Field Crops Research* 94:126-148.
- Geipel J., Link J., Claupein W. (2014) Combined spectral and spatial modeling of corn yield based on aerial images and crop surface models acquired with an unmanned aircraft system. *Remote Sensing* 6:10335-10355.
- Gitelson A.A. (2004) Wide dynamic range vegetation index for remote quantification of biophysical characteristics of vegetation. *Journal of plant physiology* 161:165-173.
- Goswami S., Gamon J., Vargas S., Tweedie C. (2015) Relationships of NDVI, Biomass, and Leaf Area Index (LAI) for six key plant species in Barrow, Alaska, PeerJ PrePrints.
- Gutierrez M., Reynolds M.P., Raun W.R., Stone M.L., Klatt A.R. (2010) Spectral water indices for assessing yield in elite bread wheat genotypes under well-irrigated, water-stressed, and high-temperature conditions. *Crop Science* 50:197-214.
- Haboudane D., Miller J.R., Pattey E., Zarco-Tejada P.J., Strachan I.B. (2004) Hyperspectral vegetation indices and novel algorithms for predicting green LAI of crop canopies: Modeling and validation in the context of precision agriculture. *Remote sensing of environment* 90:337-352.
- Jones H.G., Vaughan R.A. (2010) *Remote sensing of vegetation: principles, techniques, and applications* Oxford university press.
- Li W., Niu Z., Chen H., Li D., Wu M., Zhao W. (2016) Remote estimation of canopy height and aboveground biomass of maize using high-resolution stereo images from a low-cost unmanned aerial vehicle system. *Ecological Indicators* 67:637-648.
- Marcial-Pablo M.d.J., Gonzalez-Sanchez A., Jimenez-Jimenez S.I., Ontiveros-Capurata R.E., Ojeda-Bustamante W. (2019) Estimation of vegetation fraction using RGB and multispectral images from UAV. *International journal of remote sensing* 40:420-438.
- Montes J., Technow F., Dhillon B., Mauch F., Melchinger A. (2011) High-throughput non-destructive biomass determination during early plant development in maize under field conditions. *Field Crops Research* 121:268-273.

- Mutanga O., Skidmore A.K. (2004) Narrow band vegetation indices overcome the saturation problem in biomass estimation. *International journal of remote sensing* 25:3999-4014.
- Osborne S., Schepers J.S., Francis D., Schlemmer M.R. (2002) Use of spectral radiance to estimate in-season biomass and grain yield in nitrogen-and water-stressed corn. *Crop Science* 42:165-171.
- Prabhakara K., Hively W.D., McCarty G.W. (2015) Evaluating the relationship between biomass, percent groundcover and remote sensing indices across six winter cover crop fields in Maryland, United States. *International Journal of Applied Earth Observation and Geoinformation* 39:88-102.
- Qi J., Chehbouni A., Huete A., Kerr Y., Sorooshian S. (1994) A modified soil adjusted vegetation index. *Remote sensing of environment* 48:119-126.
- Rouse Jr J.W., Haas R., Schell J., Deering D. (1974) Monitoring vegetation systems in the Great Plains with ERTS.
- Royo C., Aparicio N., Villegas D., Casadesus J., Monneveux P., Araus J. (2003) Usefulness of spectral reflectance indices as durum wheat yield predictors under contrasting Mediterranean conditions. *International Journal of Remote Sensing* 24:4403-4419.
- Shi Y., Thomasson J.A., Murray S.C., Pugh N.A., Rooney W.L., Shafian S., Rajan N., Rouze G., Morgan C.L., Neely H.L. (2016) Unmanned aerial vehicles for high-throughput phenotyping and agronomic research. *PloS one* 11:e0159781.
- Smith G.M., Milton E.J. (1999) The use of the empirical line method to calibrate remotely sensed data to reflectance. *International Journal of remote sensing* 20:2653-2662.
- Suttie J.M., Reynolds S.G. (2004) Fodder oats: a world overview Food & Agriculture Org.
- Teal R., Tubana B., Girma K., Freeman K., Arnall D., Walsh O., Raun W. (2006) In-season prediction of corn grain yield potential using normalized difference vegetation index. *Agronomy Journal* 98:1488-1494.
- Thenkabail P.S., Smith R.B., De Pauw E. (2000) Hyperspectral vegetation indices and their relationships with agricultural crop characteristics. *Remote sensing of Environment* 71:158-182.
- Tucker C.J., Slayback D.A., Pinzon J.E., Los S.O., Myneni R.B., Taylor M.G. (2001) Higher northern latitude normalized difference vegetation index and growing

season trends from 1982 to 1999. *International journal of biometeorology* 45:184-190.